# Feasibility of Time-Lapse Surface Seismic for $CO_2$ Monitoring: A Case Study from the Decatur CCS Site, Illinois, United States

Shuvajit Bhattacharya[1], Sujith Swaminadhan[1], and Sahar Bakhshian[1,2]

[1]Bureau of Economic Geology, The University of Texas at Austin

[2]Department of Earth, Environmental and Planetary Sciences, Rice University (formerly at Bureau of Economic Geology, The University of Texas at Austin)

To whom correspondence should be addressed: Shuvajit.bhattacharya@beg.utexas.edu

# Feasibility of Time-Lapse Surface Seismic for $CO_2$ Monitoring: A Case Study from the Decatur CCS Site, Illinois, United States

Shuvajit Bhattacharya[1], Sujith Swaminadhan[1], and Sahar Bakhshian[1,2]

[1]Bureau of Economic Geology, The University of Texas at Austin

[2]Department of Earth, Environmental and Planetary Sciences, Rice University (formerly at Bureau of Economic Geology, The University of Texas at Austin)

Shuvajit.bhattacharya@beg.utexas.edu

**ABSTRACT**

We study the feasibility of time-lapse surface seismic to detect and monitor $CO_2$ plume movement over the time at the onshore Decatur CCS site, United States. We develop and test a workflow, integrating results from subsurface characterization, dynamic flow simulation, rock physics, time-lapse fluid saturation logs, and operational information to model surface seismic responses of the $CO_2$-saturated Mt. Simon sandstone reservoir over the time. We perform fluid substitution modeling under both uniform and patchy mixing conditions. Results show that 4D surface seismic responses for the Mt. Simon reservoir are weak under the historic 1 Mt of $CO_2$ injection, regardless of rock physics modeling constraints. Our modeled data under a hypothetical 10 Mt of $CO_2$ injection improves the detectability of 4D surface seismic to detect $CO_2$ plume boundary.

**KEYWORDS**

Time-lapse seismic monitoring; Rock physics; Petrophysics; Dynamic flow simulation; Carbon sequestration

## INTRODUCTION

Time-lapse seismic has been widely used in $CO_2$ monitoring over decades with an overall mixed success, for example, Sleipner $CO_2$ storage project in the North Sea (Chadwick et al., 2009), Cranfield CO2-EOR site in the United States (Zhang et al., 2013), and Quest CCS site in Canada (Harvey et al., 2022), etc. The underlying hypothesis is that the injection of a sufficient volume of $CO_2$ in the reservoir would affect acoustic impedance and seismic reflection characteristics that can be expressed via changes in seismic amplitude, time shift, polarity reversal, and quality factor, etc. Several multi-physics synthetic and site-specific $CO_2$ monitoring studies have been conducted over time. Wang et al. (2018) investigated a relationship between seismic survey parameters and the sensitivity of 2D surface seismic methods to detect a small $CO_2$ plume. Arts et al. (2009) conducted forward seismic (acoustic and elastic) modeling at the Sleipner $CO_2$ storage site in Norway and compared the modeled data with field time-lapse seismic data to detect $CO_2$ plume in the reservoir. Ajo-Franklin et al. (2013) used cross-well seismic to delineate the boundary of the $CO_2$ plume in the Frio sandstone reservoir on the Gulf Coast, Texas. Beyond seismic, time-lapse resistivity (Bergmann et al., 2012), time-lapse micro-gravity (Bonneville et al., 2021), distributed temperature sensing or DTS (Mawalkar et al., 2019), and distributed acoustic sensing or DAS (Bhakta et al., 2022) have been used in various storage reservoirs in Germany, Norway, United States, etc. for $CO_2$ plume monitoring.  Because each geophysical technique has its own resolution limits and uncertainties, researchers also studied joint inversion of multi-resolution and multi-physics data. For example, Gasperikova et al. (2022) studied the time-lapse joint inversion of seismic, resistivity, and gravity data for plume monitoring with high-fidelity. Yao et al. (2024) proposed $CO_2$ plume imaging by joint tomographic inversion using DAS and DTS data. Bukar et al. (2024) recently studied the 4D seismic time-shift attributes to understand the $CO_2$ migration along faults in the Decatur site.

Regardless of the numerous case studies on $CO_2$ plume monitoring, the broader questions remain regarding the overall effectiveness of geophysical data, specifically 4D surface seismic, in continuous $CO_2$ plume monitoring over 100 years. Are the $CO_2$ plume movement and leakage seismically detectable? Is it cost-effective? What are the technical challenges? These are valid concerns because the CCS business today is a low-profit margin business, especially if we do not consider any government subsidies and do not utilize the stored $CO_2$ in some form to sell it as a commodity, for example, manufacturing of carbon ore as feedstock and recovery of residual hydrocarbons from depleted reservoirs. However, CCS technology is important for decarbonization, with the inherent need for subsurface monitoring and verification to assure the stakeholders (including the public) of $CO_2$ plume stabilization, no leakage of $CO_2$ and brine, and no contamination of underground sources of drinking water (USDW). Cost-effective, repeatable, and fit-for-purpose monitoring tools are needed for societal acceptance, not necessarily the highest resolution tools. There are practical instances where operators may decide to acquire several 2D seismic lines, instead of a dense 3D seismic survey to reduce the cost and time of data acquisition and processing for quick screening. As new CCS field projects are announced regularly, many of which with the goal of storing gigatons of $CO_2$ in the subsurface safely over decades, it is essential to analyze the effectiveness of time-lapse seismic or any geophysical data in the study area (area of review, AOR) before, during, and after $CO_2$ injection.

Geophysical data collected for plume monitoring are just proxies that we can use to interpret the subsurface changes over time. There are several uncertainties in the correct interpretation of the plume boundary and dynamics due to geophysical survey repeatability (e.g., variations in survey design, equipment, and ground conditions, etc.), variable signal-to-noise ratio (SNR), understanding of rock-fluid-cement interaction, etc. Land seismic data quality varies dramatically due to a complex interplay of near-surface geology, variable ground conditions (e.g., snow cover, tropical storms, soil moisture, water table, etc.), spatial sampling and surface cultural changes over time. Therefore, we cannot recommend a one-size-fits-all data acquisition approach to $CO_2$ plume monitoring. Another practical challenge lies with legacy 2D/3D seismic (acquired over a decade ago), sometimes used as the baseline data. The use of such data and comparison with the future time-lapse data at the site can result in 'false positives' in interpreting $CO_2$ plume. Therefore, establishing proper baseline data is necessary.

We must analyze the effectiveness of geophysical data for monitoring by pre-injection characterization, simulation, and sensitivity studies of various data acquisition, operational, and geologic parameters. In this study, we develop and test an integrated workflow to better understand the feasibility of time-lapse surface seismic for $CO_2$ plume detection and optimization of injected $CO_2$ volume at the Decatur CCS site in Illinois, United States. The Mt. Simon reservoir (sandstone) at the Decatur CCS site underwent an injection of ~1 Mt of $CO_2$ over three years (2011-2014). Our workflow integrates site-specific geologic characterization, dynamic flow simulation, rock physics, and seismic forward modeling under different scenarios of $CO_2$ injection. Such workflow facilitates better design of $CO_2$ storage programs and monitoring designs at the site-specific boundary conditions. We also provide Madagascar programing codes for time-lapse rock physics modeling and seismic simulation in the Appendix.

The study is divided into a few major parts: subsurface characterization and building of 3D geologic models, dynamic flow simulation, rock physics modeling, and time-lapse seismic forward modeling.

## DATA

The Decatur CCS site in Illinois is a part of the US Department of Energy-funded The Illinois Basin–Decatur Project (IBDP), led by the Illinois State Geological Survey. It is an integrated carbon capture and storage project. The site underwent CO2 injection of ~1 Mt over a three-year time period (2011-2014). The project collected key data from the surface and subsurface for regional characterization, pilot studies, and CCS demonstration, many of which are made available to the public through the NETL-EDX program: https://edx.netl.doe.gov/group/illinois-basin-decatur-project. A pre-built Petrel™ software project is also publicly available with additional information from the NETL-EDX portal. Post-injection monitoring at the Decatur site was done in 2014-2021. We use publicly available baseline 3D seismic, well logs (open hole and cased hole logs, including Pulsed Neutron Capture [PNC] logs from injection and monitoring wells), $CO_2$ injection data, and other relevant information in this study. Data from one injection well (CCS #1) and one monitoring well (VW #1) was used in this study. The injection and observation wells are ~960 ft away from each other. We use the depth-converted post-stack baseline 3D seismic data in this study. The dataset was cropped to ensure efficient quality control.

We did not find the time-lapse surface 3D seismic data suitable for our study due to various acquisition and processing issues; therefore, we discarded them. We also had access to time-lapse vertical seismic profile (VSP) data, but the data had challenges due to high NRMS and different ground conditions during data acquisition (explained further in the results and discussions).

## REGIONAL GEOLOGY OF THE DECATUR CCS SITE

Several studies have been published on the local and regional geology of the Decatur CCS site in the Illinois Basin. The Illinois Basin is an intracratonic sedimentary basin. The sedimentary deposits in the basin are thick and deep near the center of the basin, similar to other intracratonic basins, such as the Michigan and Williston basins in the United States. **Figure 1** shows the generalized stratigraphy of the study area. The Mt. Simon Formation (reservoir for carbon storage) overlies the Argenta Formation and Precambrian basement. The Mt. Simon Formation is a regionally extensive sedimentary deposit throughout the US Midwest. The formation is vertically heterogeneous that can be divided into upper, middle, and lower Mt. Simon. Some portions in the lower Mt. Simon have higher porosity than middle and upper Mt. Simon, attributed to diagenetic impact (Freiburg et al., 2014; Greenberg, 2021). The facies of the lower Mt. Simon are a mixture of several depositional environments that include subaqueous coast, subaerial coast, lagoon, river, and eolian environment (Freiburg et al., 2014).

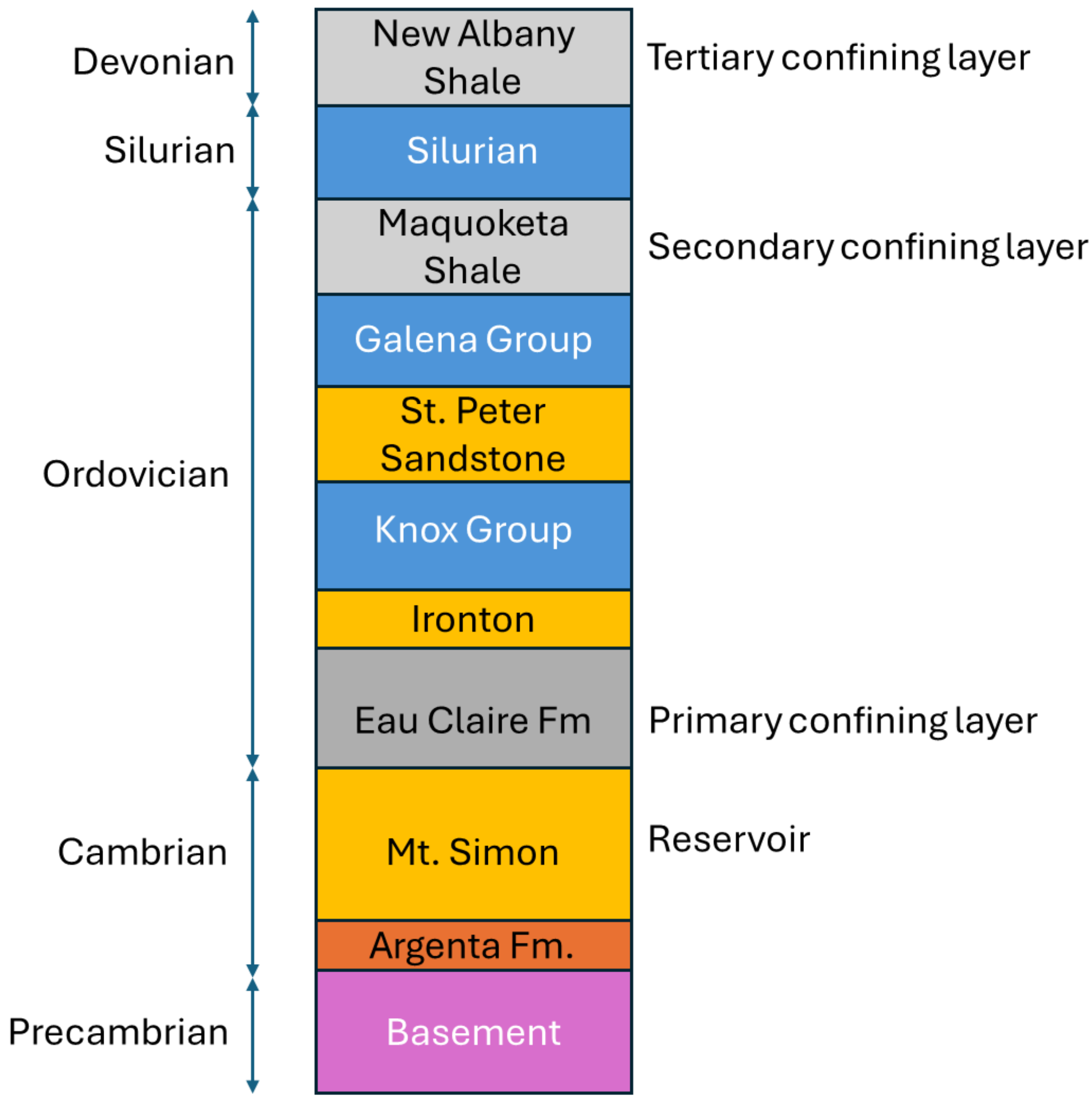


**Figure 1.** Generalized stratigraphic column (Precambrian-Devonian section) of the study area, showing the $CO_2$ storage reservoir and several confining layers (modified after Greenberg, 2021).

$CO_2$ injection was done in the Mt. Simon Formation, with Eau Claire (clay-rich) being one of the confining layers (**Figures 8 and 9**). Eau Claire directly overlies Mt. Simon reservoir. There are other potential confining layers at shallow depth, such as Maquoketa and New Albany shale.

## METHODS

We develop and test an integrated workflow that can be used to design an effective time-lapse surface seismic-driven $CO_2$ monitoring program. The workflow is shown in **Figure 2**.

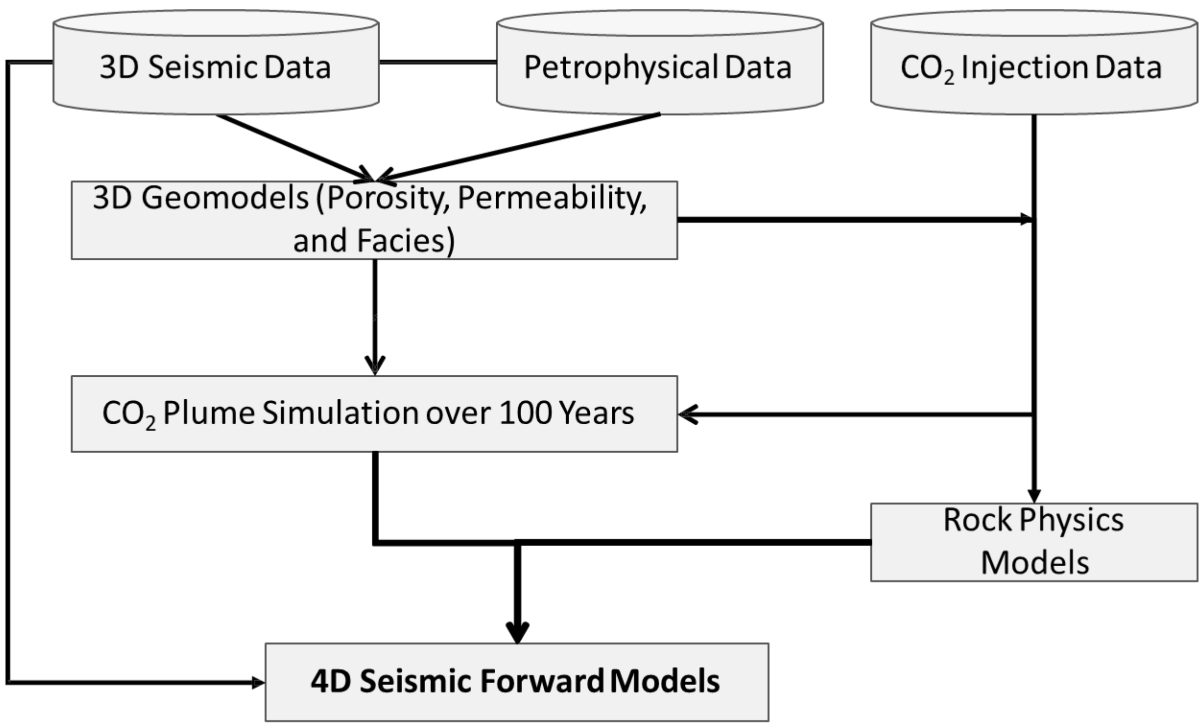


**Figure 2.** An integrated workflow used in this study (after Bhattacharya et al., 2024).

### *Geologic and Petrophysical Characterization*

We interpret well logs and core data and use the post-stack seismic inversion (P-impedance) results to map the storage window (Mt. Simon). Petrophysical analysis indicates that Mt. Simon is a saline aquifer with high porosity and permeability, therefore, high storage and flow capacity, required for $CO_2$ storage (**Figure 3**). The lower portion of the overlying Eau Claire is clay-rich, and it has low porosity and low permeability working as a confining layer. The post-stack inversion-based impedance along with core and log-based petrophysical information were used to define facies or rock types (**Figure 4**).

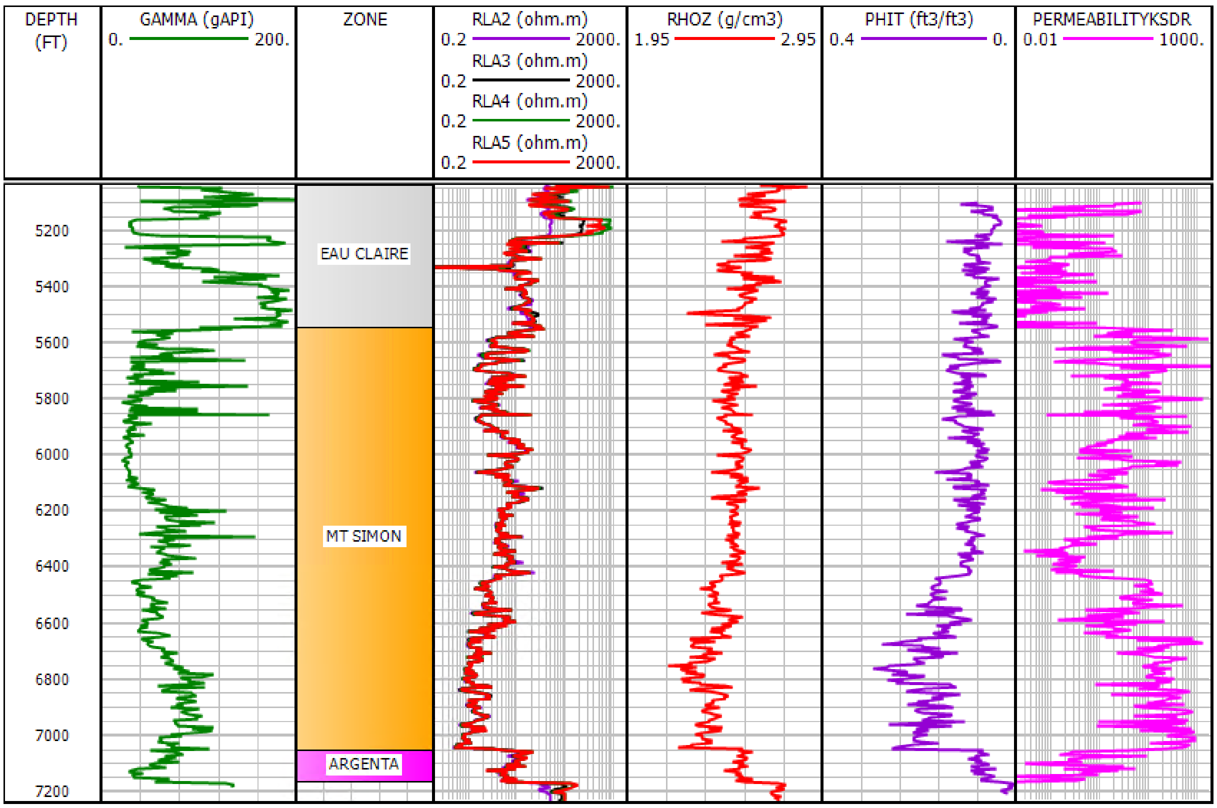


**Figure 3.** Conventional well logs from the CCS #1 well. Gamma-ray, resistivity, bulk density, derived porosity, and permeability logs are displayed in tracks 1, 3, 4, 5, and 6, respectively. $CO_2$ was injected in the lower Mt. Simon.

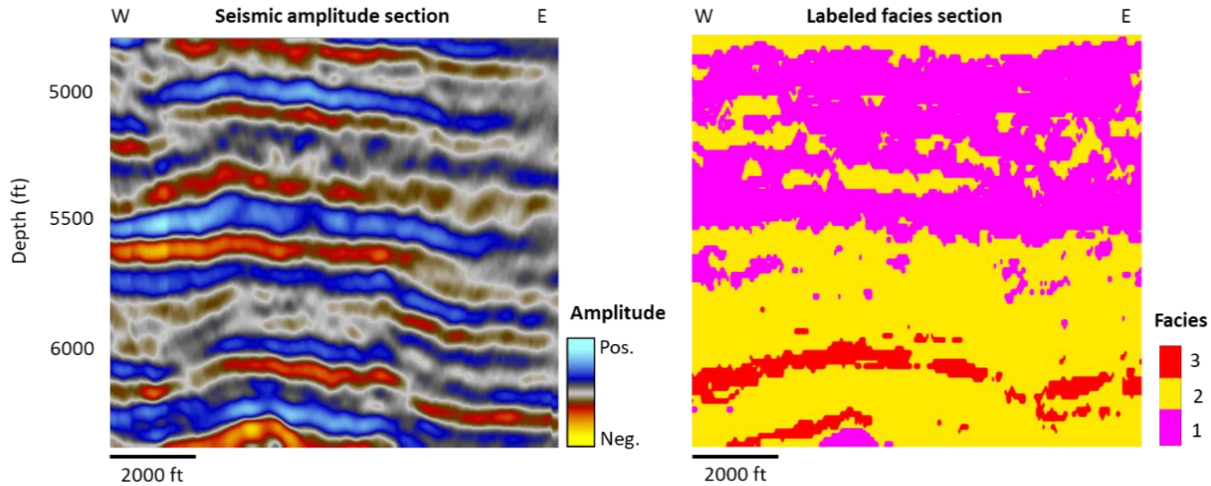


**Figure 4.** Seismic amplitude and corresponding facies (Facies 3: coarse-grained sand, Facies 2: fine-grained sand, and Facies 1: shale)

We examine the porosity, permeability, capillary pressure, and geologic facies characteristics to define rock types, in terms of and fit-for-purpose reservoir simulation. The model is composed of three rock types including coarse-grained sand (porosity higher than 20%), fine-grained sand (porosity between 10-20%), and shale (porosity less than 10%). We developed our cutoff values based on the porosity and permeability data from wells, publicly available project reports (IBDP, 2021), and relevant petrophysical knowledge, which were also verified by running multiple in-house dynamic flow simulations for $CO_2$ plume migration.

Relative permeability of coarse sand was calculated by fitting the Brooks-Corey's model (Brooks and Corey, 1964) to the experimental data reported for this rock type (Zaluski and Lee, 2019). Capillary pressure for the coarse sand was estimated using the van Genuchten model. Due to the lack of core analysis data for the fine sand and shale, we used $CO_2$-brine relative permeability and capillary pressure curves reported in Krevor et al. (2012) and Lahann et al.

(2014). To account for the contribution of $CO_2$ residual trapping, we incorporated the hysteresis characteristics into the relative permeability curves. Relative permeability and capillary pressure curves for all facies are depicted in **Figs. 5, 6, and 7.**

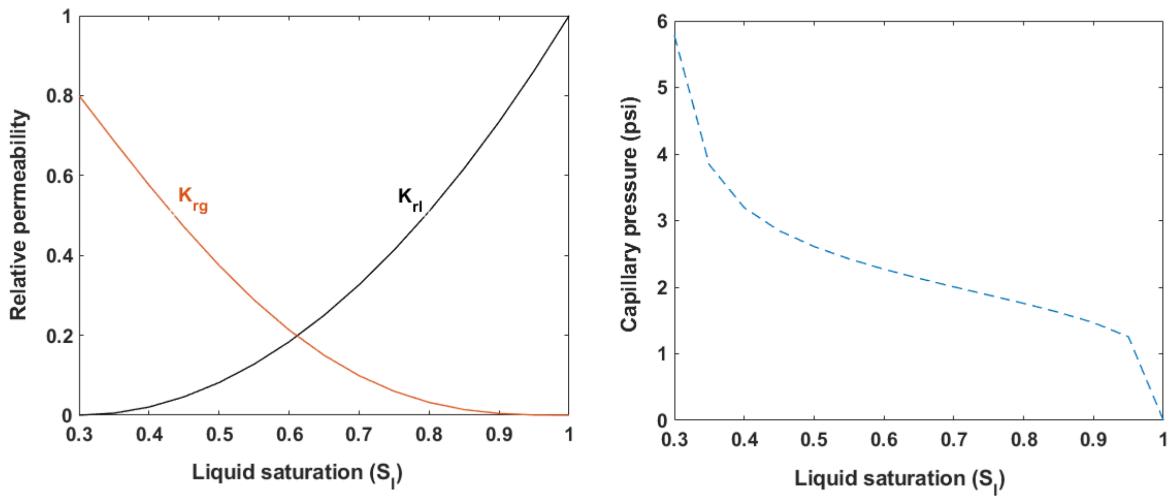


**Figure 5.** Relative permeability and capillary pressure curves for coarse-grained sand.

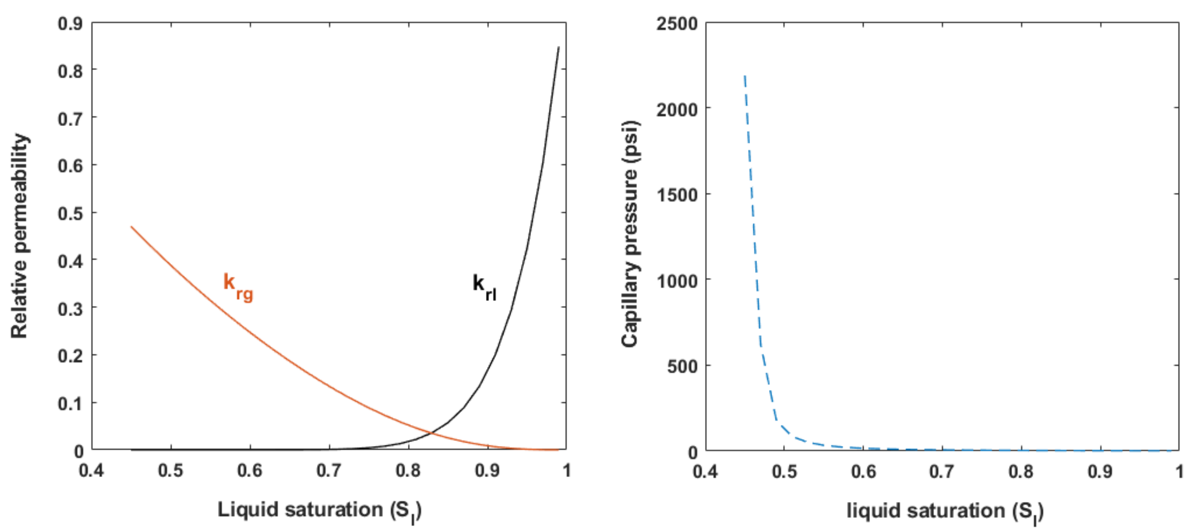


**Figure 6.** Relative permeability and capillary pressure curves for fine-grained sand.

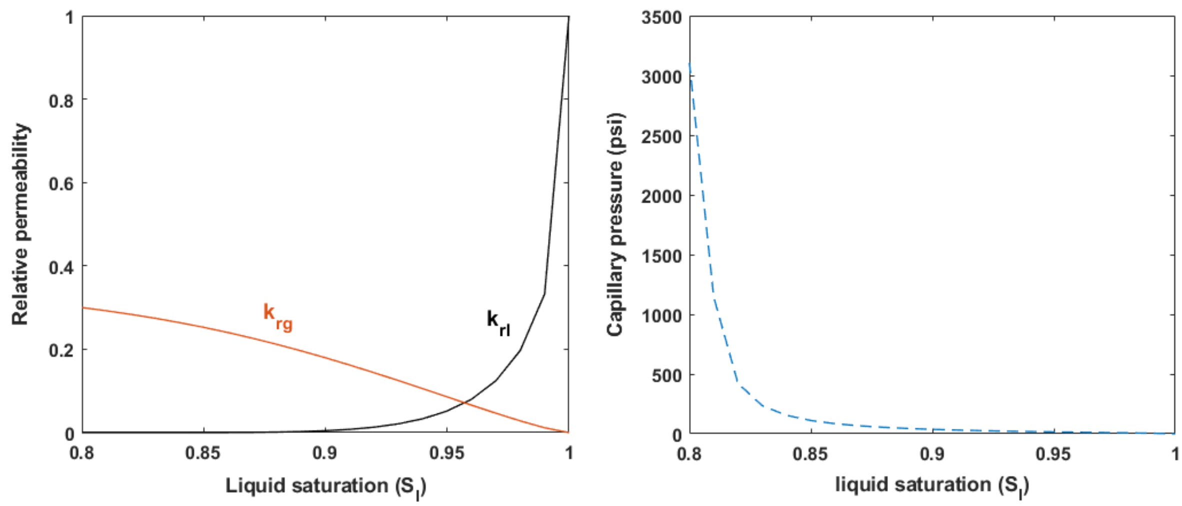


**Figure 7.** Relative permeability and capillary pressure curves for shale (baffle).

### *3D Geologic Modeling and Reservoir Flow Simulation*

We build a 3D geologic model of the $CO_2$ storage system, populated with facies, porosity, and permeability. The original geocellular 3D model developed by SLB (formerly Schlumberger) that is publicly available contains 25 million grid cells (IBDP, 201).

In order to reduce the computational complexity of multiphase flow simulations, we upscaled the geologic and reservoir property models (facies, porosity, and permeability) and also cropped a portion of the underlying confining zone below the Mt. Simon reservoir that does not contribute to $CO_2$ plume migration. Through those modifications, the number of grid cells in the models was reduced to 5 million. The updated porosity, permeability, and facies models (which were used as input to dynamic flow simulation and seismic modeling) are shown in **Figs. 8 and 9**.

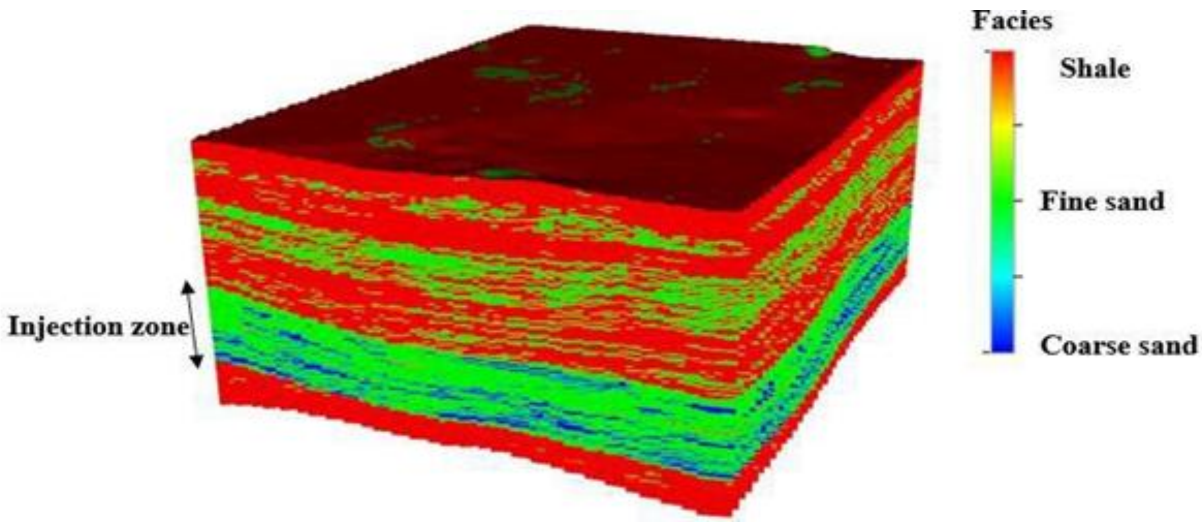


**Figure 8.** A 3D facies model of the study area, generated as a part of this study. The injection zone is shown in a double-headed arrow.

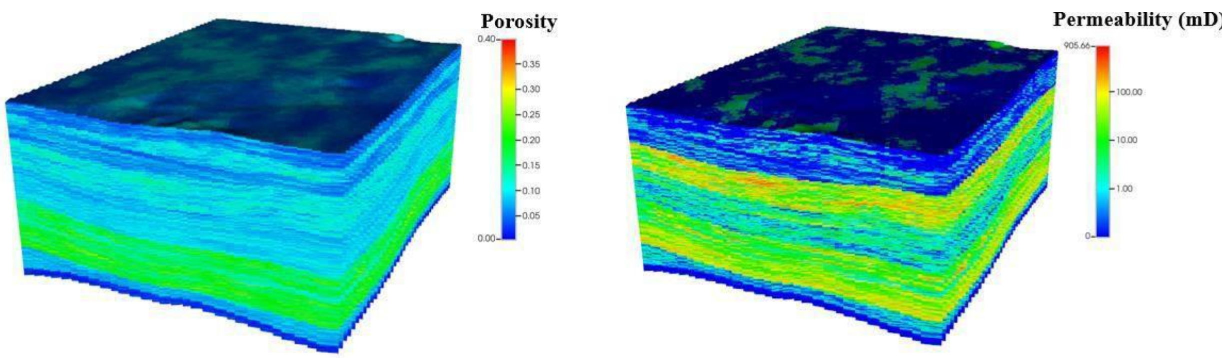


**Figure 9.** Redistributed porosity and permeability models in the study area. Upper and lower Mt. Simon have favorable reservoir properties.

We performed compositional simulations of $CO_2$ injection using the Generalized Equation of State Model Reservoir Simulator (GEM) from the CMG-Computer Modeling Group (CMG, 2021). $CO_2$ was injected through CCS #1 well (**Figure 10**) into the Mt. Simon Formation, with a maximum well bottom-hole pressure (BHP) of 4,896 psi. The maximum BHP is considered to be

80% of the rock fracture pressure (Bakhshian et al., 2023). $CO_2$ injection was performed from November 2011 to November 2014, followed by post-injection monitoring until 2100.

In addition to using the historical $CO_2$ injection data, we also simulated for a hypothetical 10 Mt of $CO_2$ injection over three years. We do not consider any poro-elastic and geochemical changes as a part of the simulation and corresponding seismic feasibility studies. **Figs. 10 and 11** represent side, top, and 3D view of the $CO_2$ saturation plume at the end of injection and post injection for 1 Mt and 10 Mt scenarios, respectively. The spatial evolution of the plume (for 1 Mt CO2 injection) is shown in **Figure 12**. After the $CO_2$ is injected, the plume is built and grown around the injection well (causing high $CO_2$ saturation). Over time, the plume migrates away from the injection well (causing low $CO_2$ saturation) and reaches one of the observation wells, which is 960 ft away.

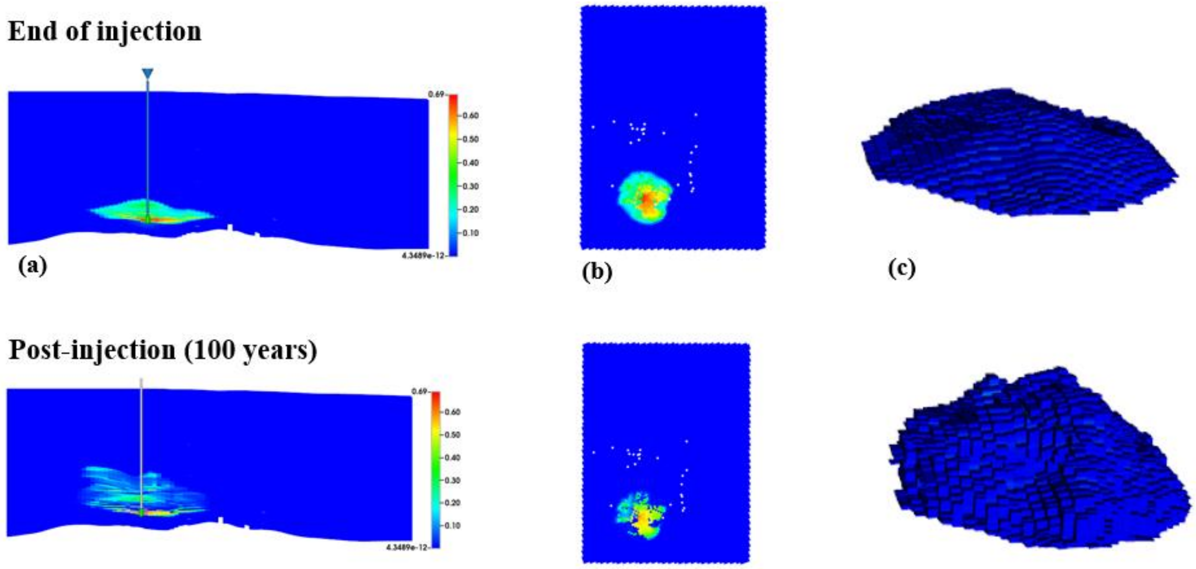


**Figure 10.** Side (a), top (b), and 3D view (c) of $CO_2$ plume at the end of $CO_2$ injection and 100 years post-injection for 1 Mt injected $CO_2$. Warm colors indicate high $CO_2$ saturation. CCS #1 well is shown in the blue vertical line.

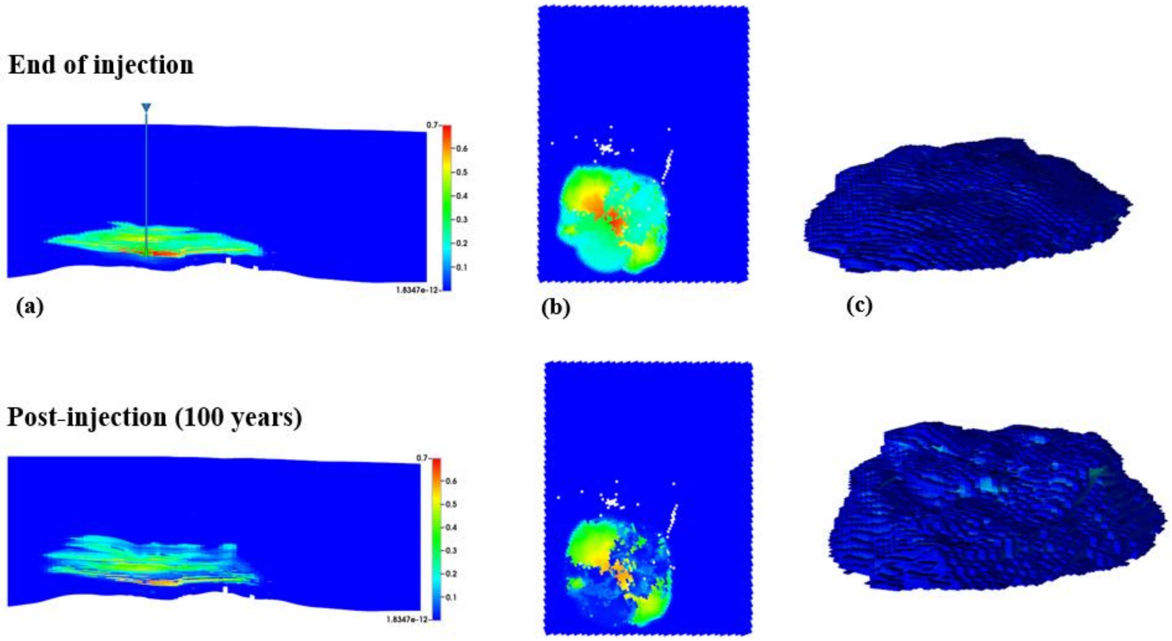


**Figure 11.** Side (a), top (b), and 3D view (c) of $CO_2$ plume at the end of $CO_2$ injection and 100 years post-injection for a hypothetical 10 Mt injected $CO_2$. Warm colors indicate high $CO_2$ saturation. CCS #1 well is shown in the blue vertical line.

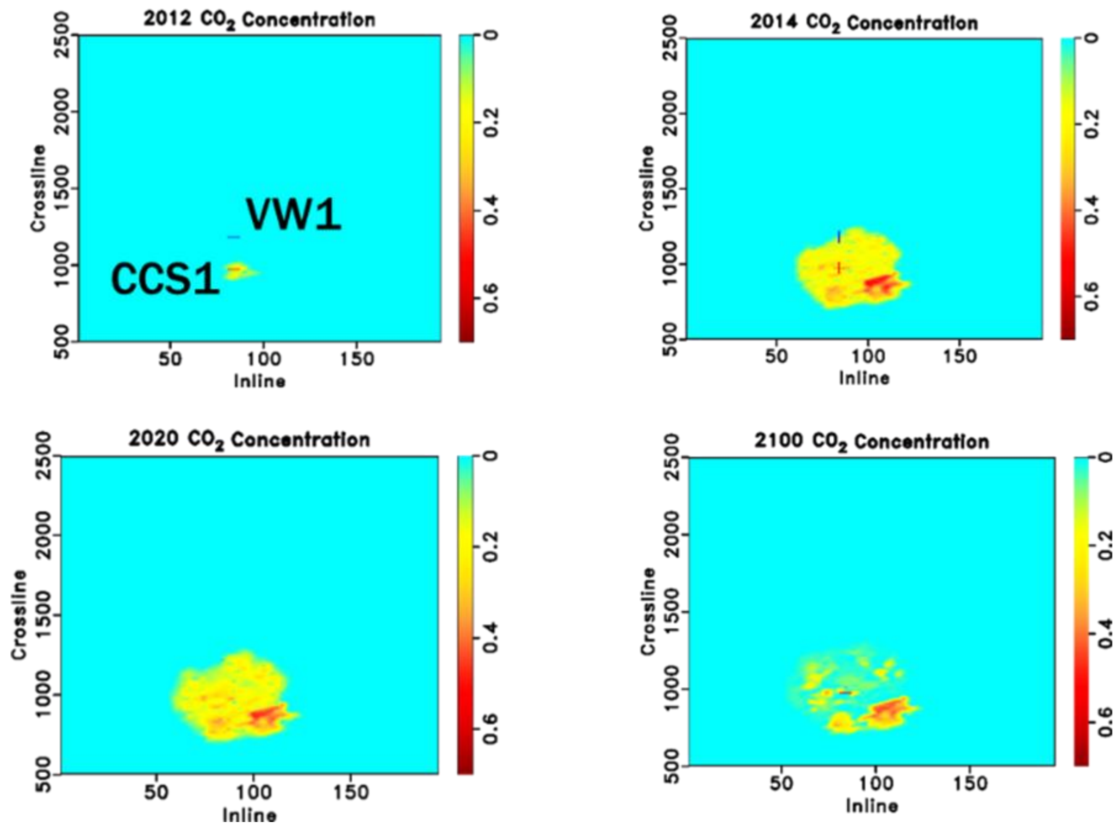


**Figure 12.** Plan view of the $CO_2$ flow simulation results (1 Mt $CO_2$ injection) over the years, starting from 2012 to 2100. Injection (CCS #1) and monitoring (VW #1) wells are shown in red and blue plus (+) symbols.

***Validation of Dynamic Flow Simulation***

We verified reservoir flow simulation results with the cased-hole Pulse Neutron Spectroscopy (PNC) log-based estimates of $CO_2$ saturation in both injection and monitoring wells for a few years from when the PNC log data are available (i.e., 2012, 2013, 2014, 2016). Note that PNC log results are only valid for the near-wellbore sections; it has a small depth of investigation. Also, background gas and wellbore integrity may deteriorate signals to an extent, thereby leading to wrong interpretations. We used the PNC results to constrain the reservoir simulation parameters, while making sure that the selected parameters were physically meaningful.

***Rock Physics Modeling***

We use the baseline and time-lapse dynamic flow simulation models in time-lapse rock physics modeling. We explore the effects of rock physics and seismic response in the context of fluid saturation models. The $CO_2$ simulation models for specific time steps 2013, 2014, 2020, 2040, and 2100 were used in seismic modeling. We use Gassmann's fluid substitution theory, with underlying assumptions, to estimate the $CO_2$-saturated rock properties and convolution modeling to retrieve the resultant seismic response (Gassmann, 1951; Kazemeini et al., 2010). We assumed no changes in reservoir properties, deposition of minerals (e.g., salt), and any chemical and geomechanical changes due to $CO_2$ injection. We generated the baseline (pre-injection) rock physics model by assuming 100% brine content in the pore space. We also explored the effect of seismic response with different frequencies.

**Figure 13** shows the pattern of velocity variation with $CO_2$ saturation under uniform and patchy mixing conditions. Under the patchy mixing condition, the velocity decreases with $CO_2$ saturation in a linear pattern, whereas the velocity shows a non-linear pattern under uniform condition. The magnitude of the change in velocity with the changes in $CO_2$ saturation under the uniform mixing condition is smaller than that of patchy mixing condition. Therefore, we may may expect high uncertainties with quantifying $CO_2$ saturation from seismic or log-based velocity information in reservoirs where unform mixing condition is fully valid. In reality, most reservoirs behave between fully uniform and patchy mixing conditions. Sonic logs, derived mineral volumes, and porosity from CCS #1 well are shown in **Figure 14**. **Table 1** shows the parameters used in the rock physics model, considering various minerals and pore fluid components, as indicated by petrophysical analysis (**Figure 14**).

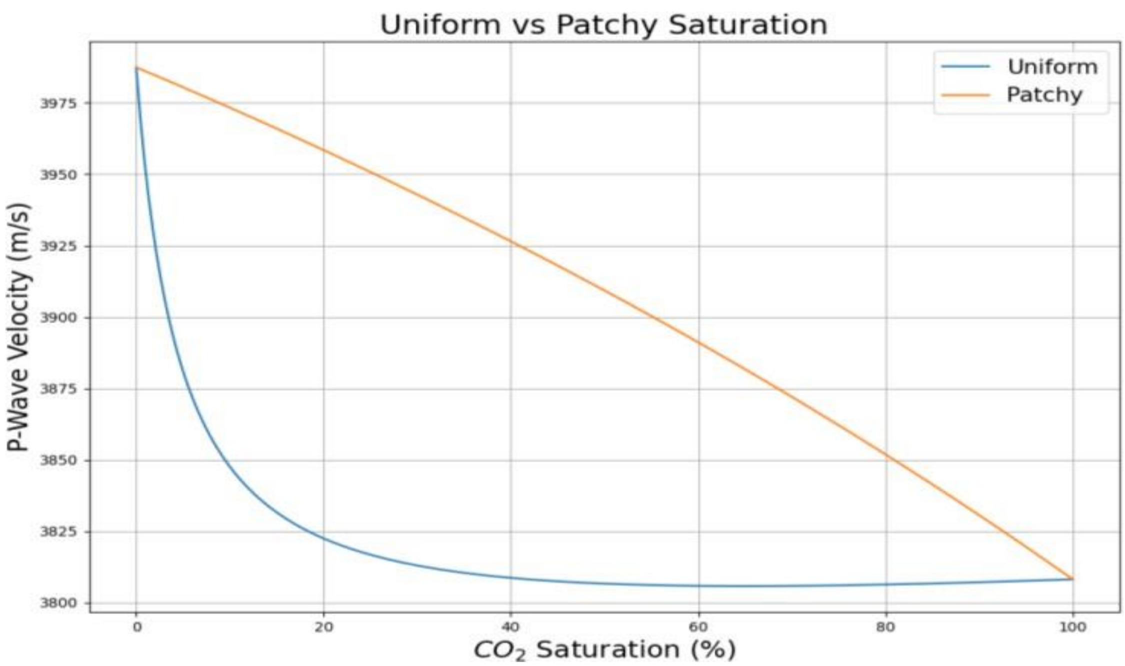


**Figure 13.** The relationship between $CO_2$ saturation and P-wave velocity under uniform and patchy mixing conditions. Note the linear (patchy) and non-linear (uniform) nature of the curves.

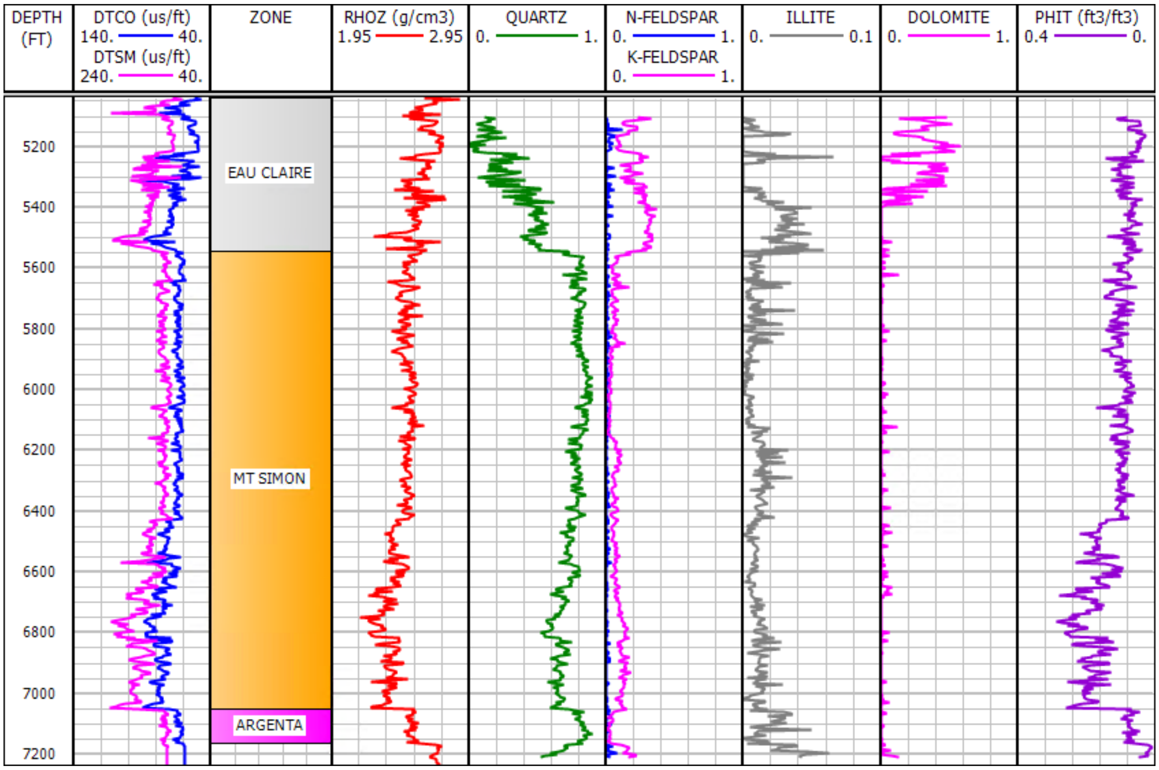


**Figure 14.** Compressional sonic (DTCO), shear sonic (DTSM), density (RHOZ), derived mineral volumes (quartz, clay, feldspar, and dolomite), and porosity (PHIT) curves from the CCS #1 well.

**Table 1.** Elastic parameters of different minerals and fluid (brine and $CO_2$) used in rock physics modeling

| Mineral/Fluid | Bulk Modulus (GPa) | Shear Modulus (GPa) | Density (g/cm$^3$) |
|---|---|---|---|
| Quartz | 37 | 44 | 2.65 |
| Feldspar | 37.5 | 15 | 2.62 |
| Dolomite | 76.4 | 49.7 | 2.87 |
| Clay | 25 | 9 | 2.55 |
| Brine | 2.3 | 0 | 1.03 |
| $CO_2$ | 0.075 | 0 | 0.70 |

***Generation of 3D Volumes of Elastic Properties***

Ideally, one would have access to pre-stack seismic and perform simultaneous inversion to derive elastic properties, such as bulk modulus, shear modulus, Vp/Vs ratio, which can be used for baseline modeling (Shoemaker et al., 2019). Since we did not have access to pre-stack multi-component seismic, we used post-stack seismic (the most common situation) and petrophysical inversion results from four wells at the Decatur CCS site as inputs to generate 3D volumes of bulk modulus, shear modulus, Vp/Vs ratio, and density, as well as 3D modeled seismic volume. We used a predictive painting approach to generate 3D volumes of rock physics properties. Predictive painting is an interpolation method based on the plane wave construction principle (Fomel, 2010; Fomel, 2016). The predictive painting was guided by smoothly varying dip (Fomel, 2002) estimated from the baseline post-stack 3D seismic data. **Figure 15** compares the seismic trace at the depth of the Mt. Simon reservoir at the location of the CCS #1 well from the original (acquired) post-tack 3D seismic and modeled 3D seismic. The correlation between these seismic traces at the reservoir interval (Mt. Simon) is generally high based on quantitative estimates as well as the visual comparison of the entire volumes. However, these two volumes are not exactly the same for the entire subsurface section due to various reasons, for example, the uncertainties with petrophysical inversion results from four wells used in predictive painting, SNR, and the effect of near-surface geology. **Figure 16** shows the derived bulk modulus, shear modulus, Vp/Vs ratio, and density volumes. Our proposed workflow shows an example of overcoming the usual challenges with the lack of above-mentioned key elastic property volumes from pre-stack seismic data, and how one can use our approach to derive these critical rock physics properties from post-stack data with reasonable resolution. We used this modeled 3D seismic as the baseline data for monitoring feasibility analysis.

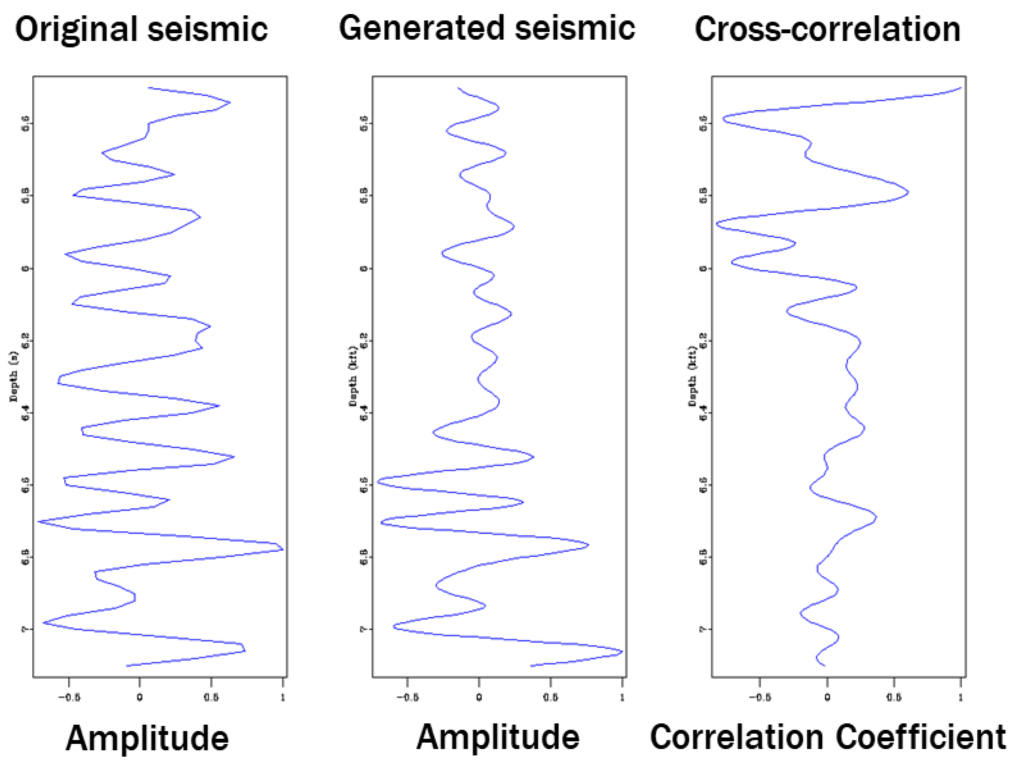


**Figure 15.** A comparison between the original seismic trace and synthetic seismic trace (after predictive painting) at the injection well (CCS #1) location, and the correlation between each trace.

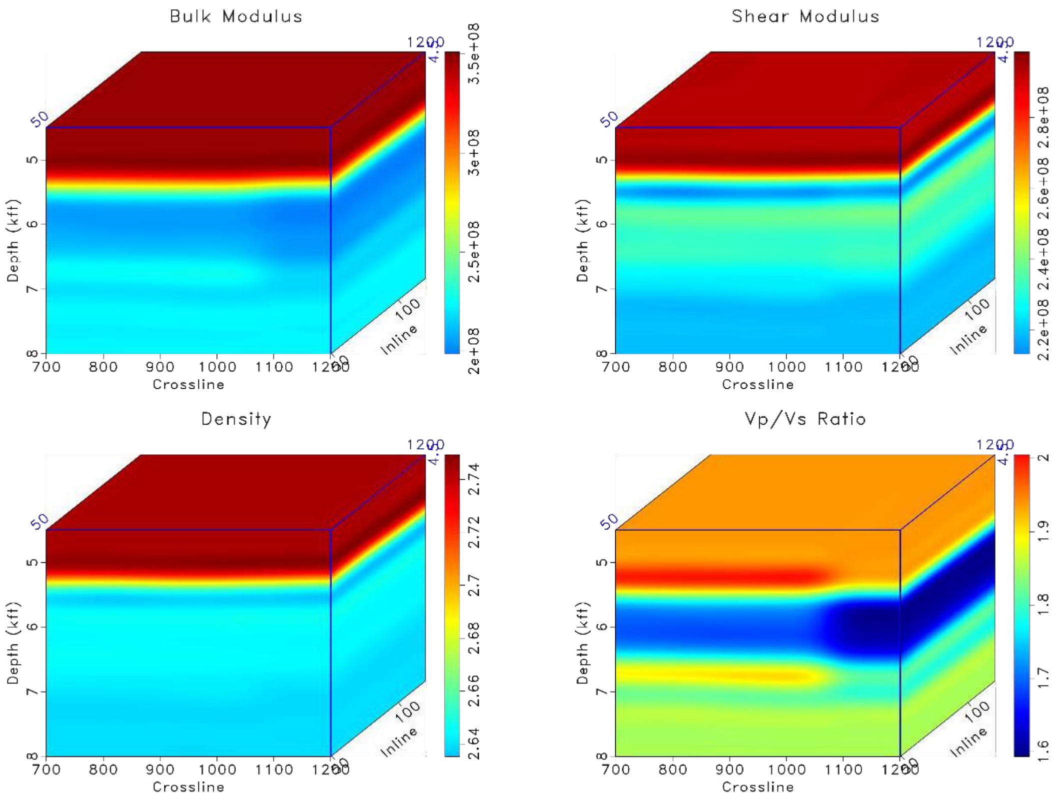


**Figure 16.** 3D volumes of bulk modulus, shear modulus, density, and Vp/Vs ratio.

### *Time-Lapse Seismic Forward Modeling*

We generate the time-lapse seismic responses by simple zero-offset convolution modeling. We estimate the reflectivity series by using the Zoeppritz equations (Zoeppritz, 1919) and used a Klauder wavelet of 15-65 Hz as the source wavelet. The choice for the Klauder wavelet is due to its resemblance to the available 3D seismic data. A baseline seismic response was generated by considering a 100% brine within the pore space of the Mt. Simon reservoir. Then, we generated time-lapse responses considering dynamic flow simulation results yielding spatio-temporal variation of $CO_2$ saturation and corresponding rock physics models under both uniform and patchy saturation models.

## RESULTS AND DISCUSSIONS

Our subsurface characterization indicates the Mt. Simon reservoir is a saline aquifer, primarily composed of sandstone with siltstone and shale, with variable porosity and permeability. Petrophysics-guided seismic inversion results indicate the lateral variability of facies and petrophysical properties. Lower Mt. Simon is highly porous and permeable, which is good for $CO_2$ storage. The dynamic flow simulation results generated using the static model parameters show the vertical and lateral movement of the plume for 2012-2100 (**Figure 17**). The lateral extent of the plume migration is limited (<1,000 ft). This is also confirmed from the available time-lapse PNC log signatures in the monitoring well (VW#1), which is ~960 ft away from the injection (CCS #1) well (**Figure 18**). The modeling results indicate that $CO_2$ stays within the Mt. Simon storage reservoir even after 80 years of post-injection. However, continuous monitoring is necessary to verify that. $CO_2$ saturations tend to be higher at those grid blocks associated with the coarse-grained sandstone with high porosity and permeability.

Time-lapse seismic forward models performed under uniform and patchy mixing conditions reveal different trends of the variation of seismic velocity with respect to the changes in $CO_2$ saturation (**Figs. 19 and 20**). For the 4D forward seismic models constructed under uniform mixing condition (with no noise in the data), we found up to 7% change in amplitude with 1 Mt. ton of $CO_2$ injection from 2100 to 2100. The overall $CO_2$ plume boundary can be somewhat detected (assuming zero noise in the data which is non-physical); however, the results deteriorate under patchy mixing conditions, with only 2% change in seismic amplitudes, making 4D seismic method ineffective in accurately detecting $CO_2$ plume in this case.

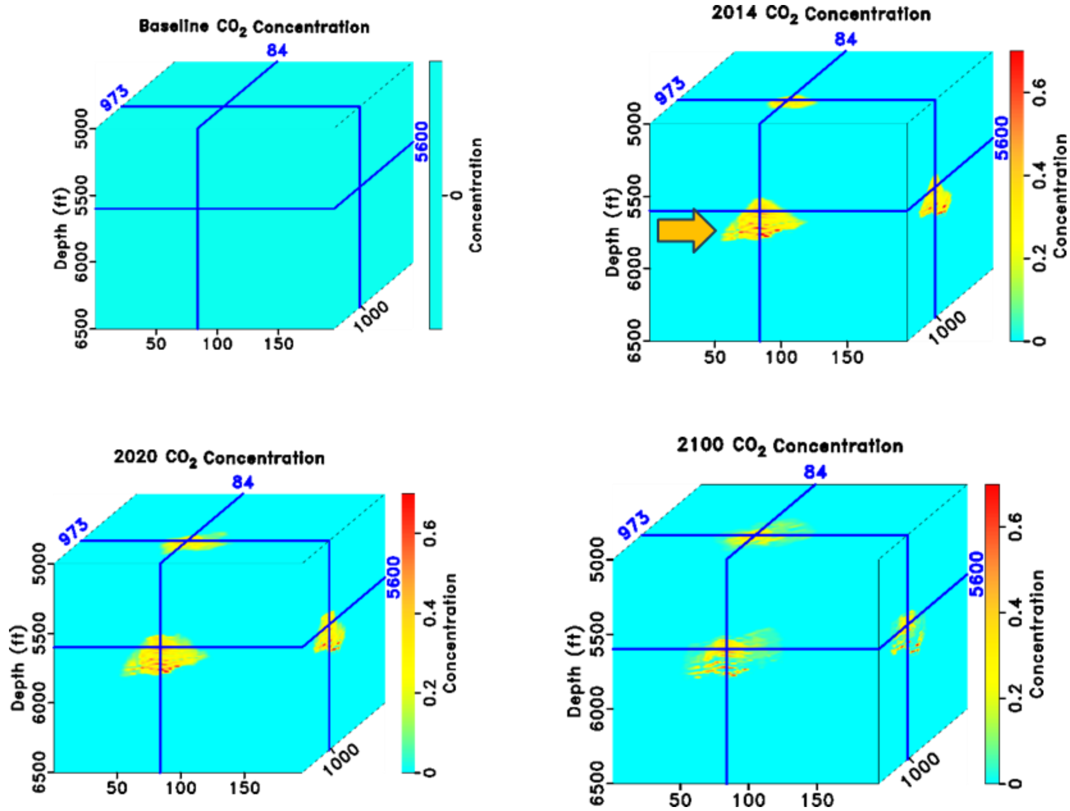


**Figure 17.** 3D volumes of $CO_2$ saturation (1 Mt injection) from dynamic flow simulation results from baseline, and three time-lapse conditions (year 2014, 2020, and 2100). Warm colors represent high $CO_2$ saturation. Blue planes illustrate the projected $CO_2$ plume distribution along inline (side view), crossline (cross-section view), and depth slice (top view) from the injection well.

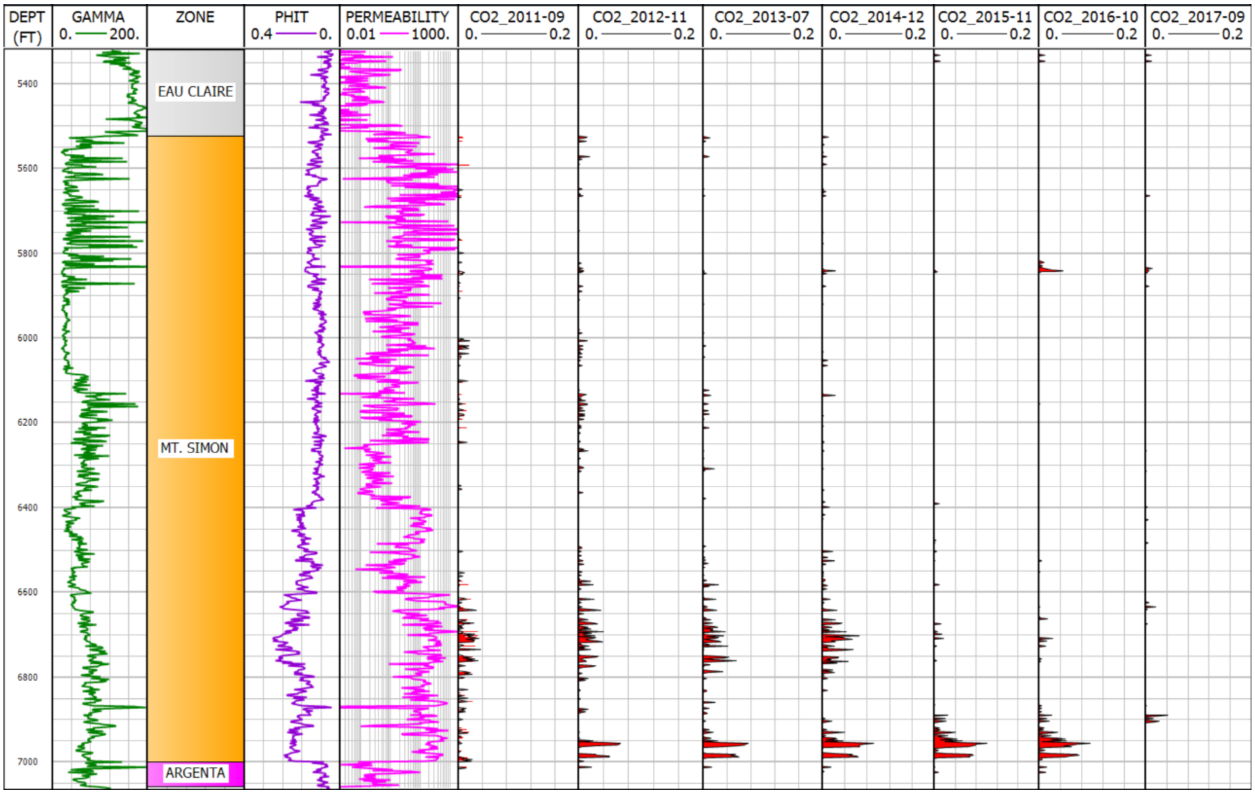


**Figure 18.** A well-log display showing the gamma-ray (track 1), zones (track 2), total porosity (track 3), permeability (track 4), and time-lapse PNC log signature at the monitoring well (VW 1) over different years (track 5-11). The limits for $CO_2$ saturation are the same for tracks 5-11, between 0 and 20%.

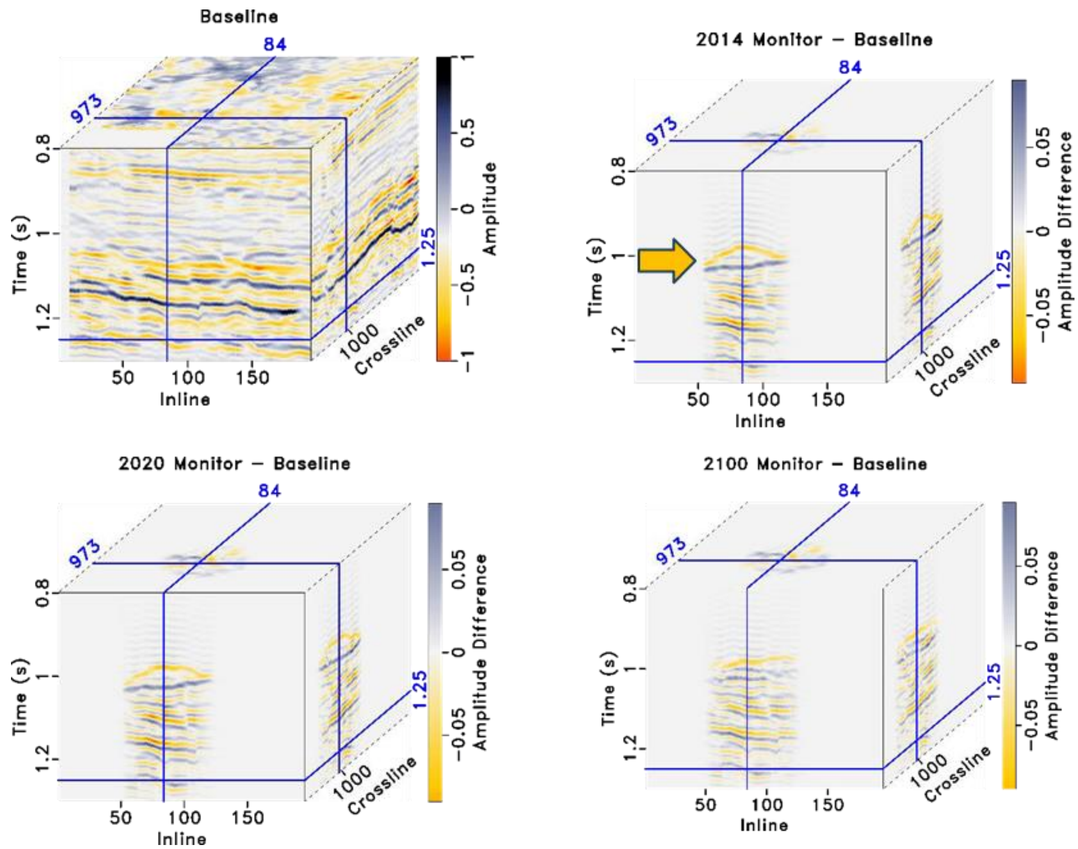


**Figure 19.** Time-lapse forward seismic models, and the amplitude differences between time-lapse and baseline data in 2014, 2020, and 2100 under uniform mixing condition and 1 Mt of injected $CO_2$, using results from Figure 17. Dark yellow arrow indicates the imaged $CO_2$ plume.

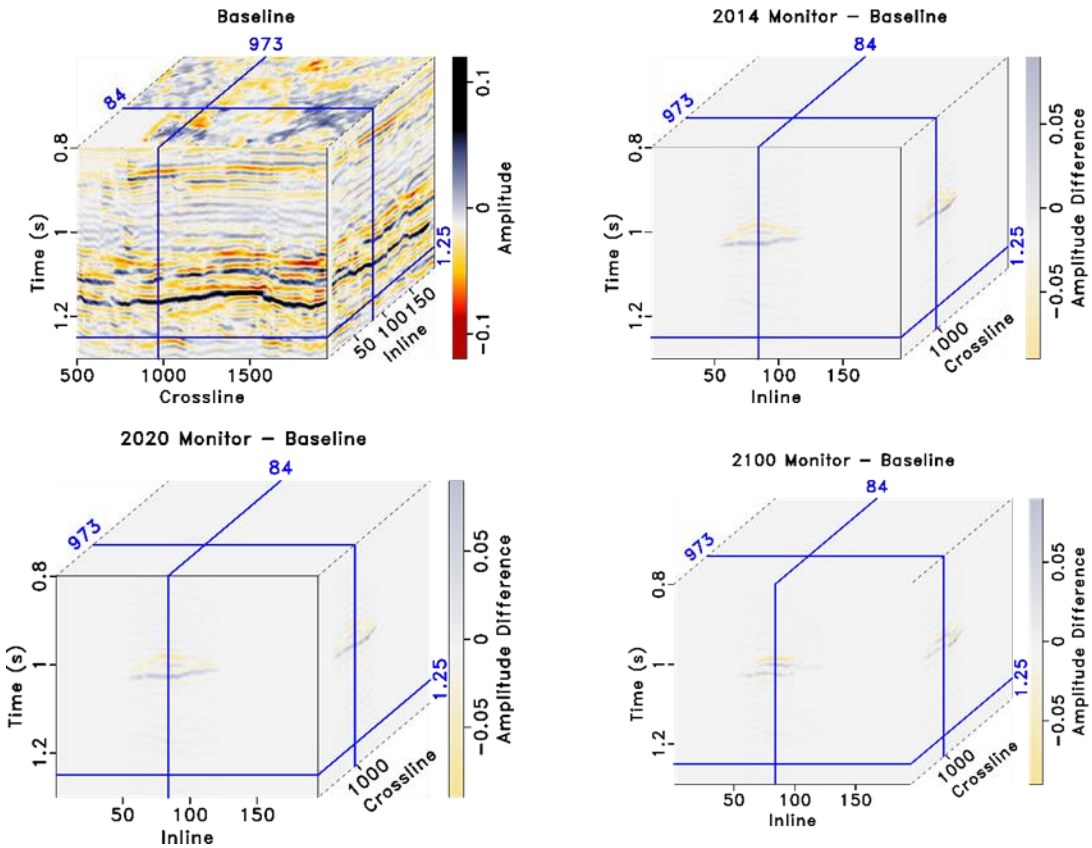


**Figure 20.** Time-lapse forward seismic models, and the amplitude difference between time-lapse and baseline data in 2014, 2020, and 2100 under patchy mixing condition and 1 Mt of injected $CO_2$, using results from Figure 17.

We compared the results from time-lapse uniform and patchy mixing models, in terms of acoustic impedance, Vp/Vs ratio, porosity, and $CO_2$ saturation (**Figure 21**). We observed a higher scatter of impedance and Vp/Vs ratio for the same porosity and $CO_2$ concentration under uniform condition than patchy mixing condition, implying a higher uncertainty in the estimated values of acoustic impedance and Vp/Vs ratio in the uniform mixing model. To quantify the uncertainty associated with the fluid saturation models, we used the running standard deviation as a metric and found that the uncertainty ranges up to 3% in the uniform mixing cases, compared to the patchy condition showing only 0.7% scatter. Regardless, we think the reservoir has some patchiness due to diagenesis, varying pore characteristics, and cementation at depth.

Since seismic amplitudes from time-lapse forward seismic models could not accurately detect $CO_2$ plume boundary, we conducted another set of experiments with the hypothesis that injecting a much higher $CO_2$ injection volume of 10 Mt over three years would result in a significant change in seismic amplitude that could be detectable in surface seismic. Dynamic flow simulation results under 10 Mt of $CO_2$ injection show the considerable spread of $CO_2$ plume laterally and vertically (**Figure 22**). 4D forward seismic models under both uniform and patchy mixing conditions showed the $CO_2$ plume boundary (**Figures 23 and 24**). NRMS amplitude metric was also estimated for each 4D seismic model under uniform and patchy mixing conditions, with 1 Mt and 10 Mt of $CO_2$ injected (**Figures 25 and 26**). NRMS ranges between 10-18% for uniform mixing, compared to 4-6% for patchy mixing.

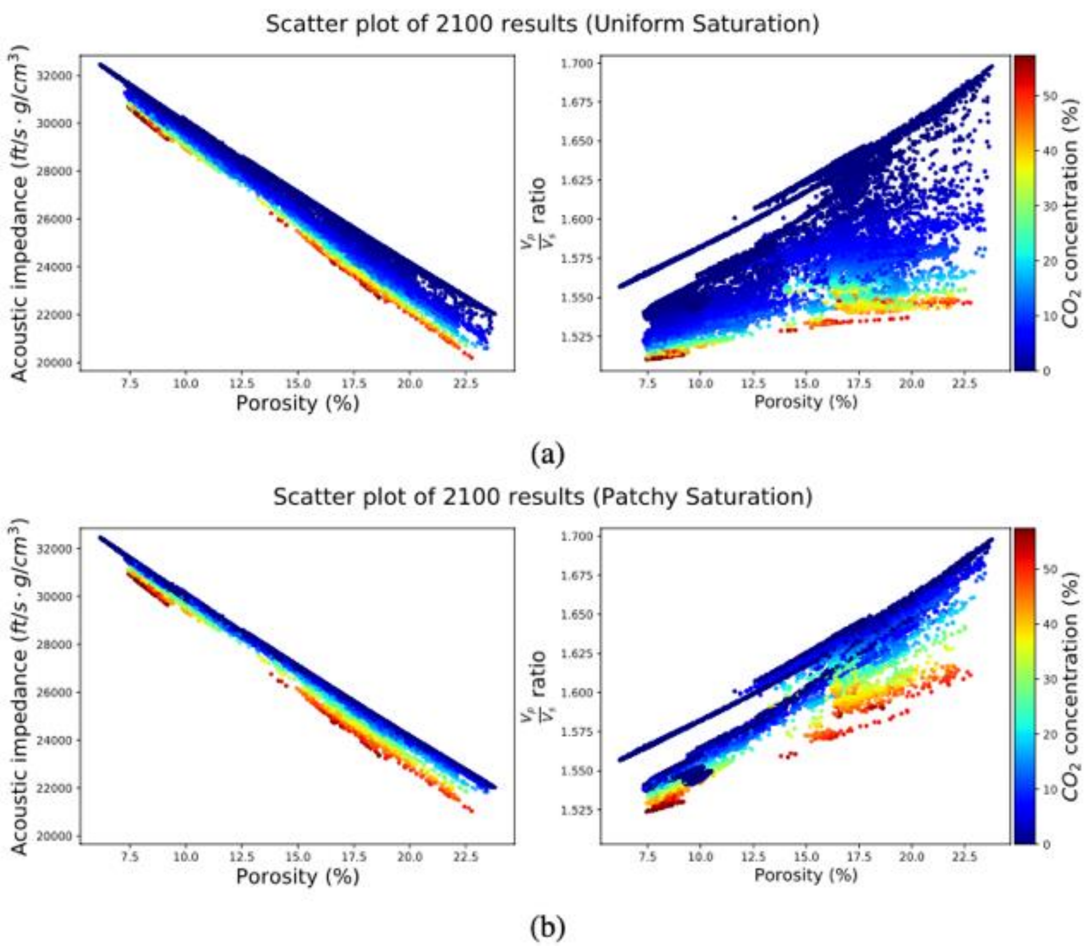


**Figure 21.** Scatter plots of acoustic impedance (left), Vp/Vs ratio (right) vs. porosity vs. $CO_2$ concentration corresponding to time-lapse seismic models at the post-injection scenario of year 2100 a) Uniform mixing model, b) Patchy mixing model. Warm colors indicate high $CO_2$ saturation.

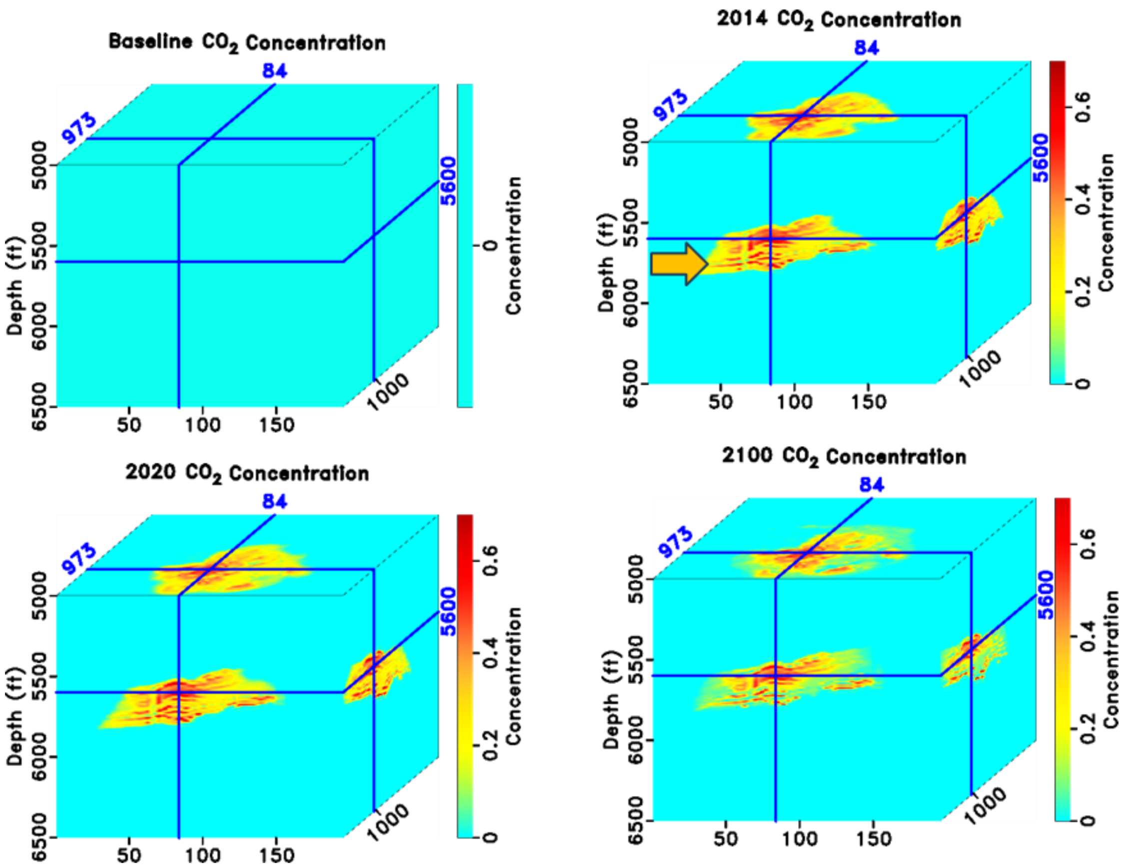


**Figure 22.** 3D volumes of $CO_2$ saturation (under hypothetical 10 Mt injection) from dynamic flow simulation results from baseline, and three time-lapse conditions (year 2014, 2020, and 2100). Warm colors represent high $CO_2$ saturation. Blue planes illustrate the projected $CO_2$ plume distribution along inline (side view), crossline (cross-section view), and depth slice (top view) from the injection well.

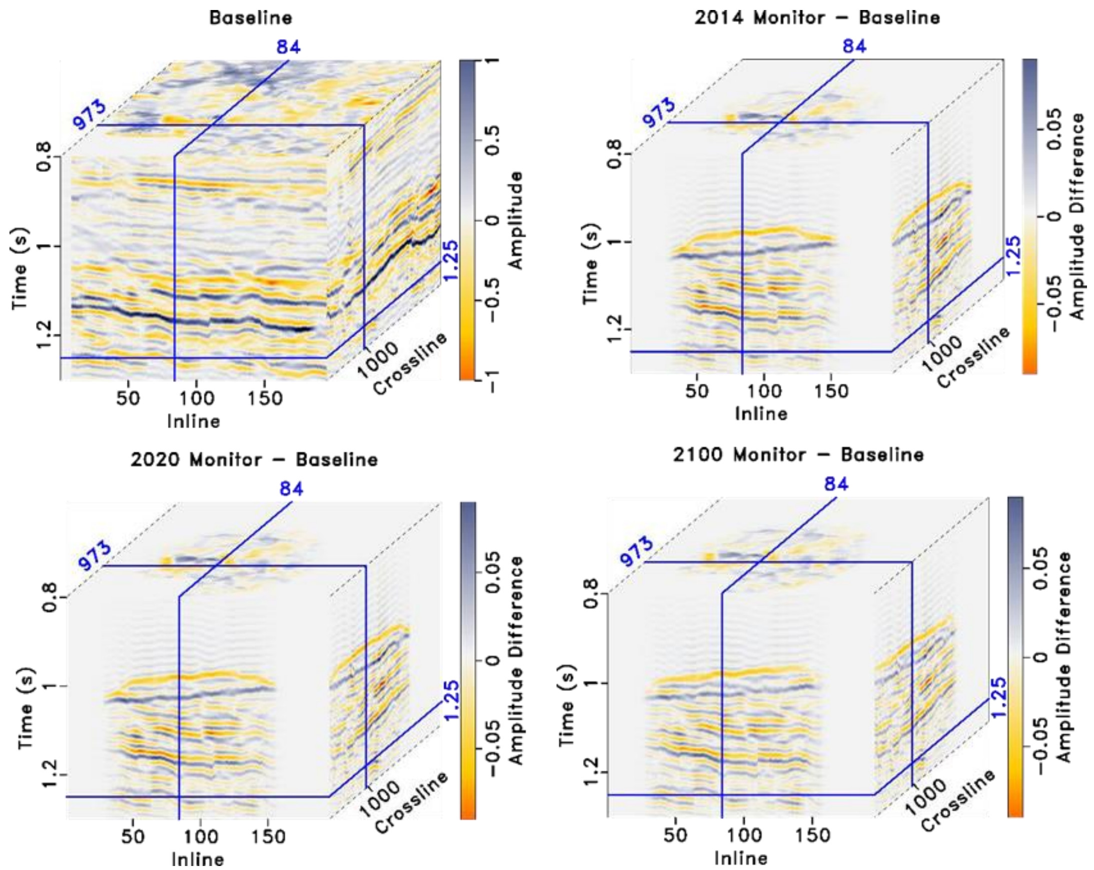


**Figure 23.** Time-lapse forward seismic models, and the amplitude difference between time-lapse and baseline data in 2014, 2020, and 2100 under uniform mixing condition and 10 Mt of $CO_2$, using results from Figure 22.

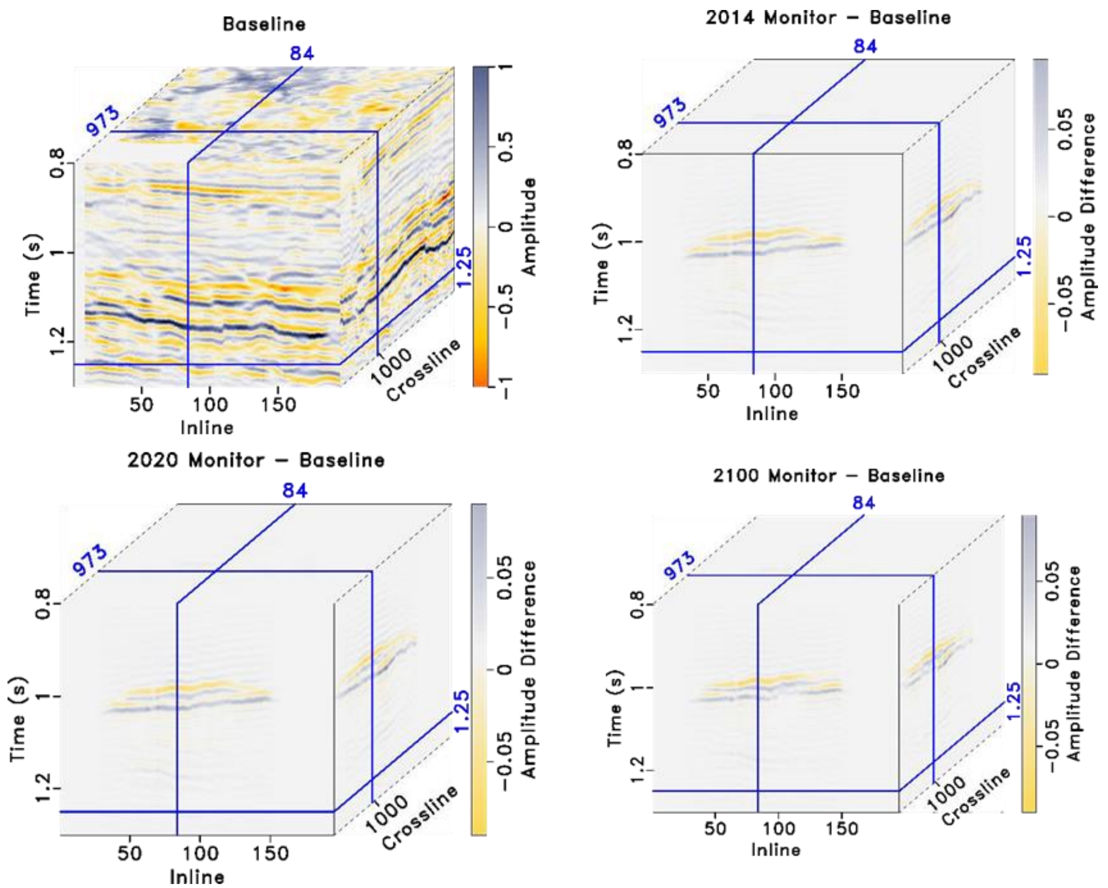


**Figure 24.** Time-lapse forward seismic model, and the amplitude difference between time-lapse and baseline data in 2014, 2020, and 2100 under patchy mixing condition and 10 Mt of $CO_2$, using results from Figure 22.

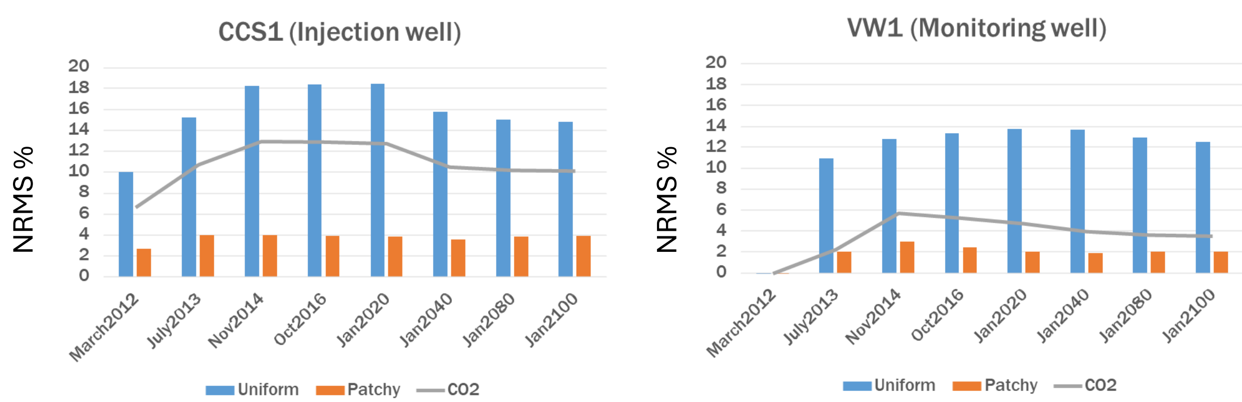

**Figure 25.** NRMS values in the injection and monitoring wells over the years under uniform and patchy mixing conditions for a 1 Mt of $CO_2$ injection. The grey line indicates the percentage change in the $CO_2$ saturation at the injection (left) and monitoring (right) wells, compared to the baseline condition.

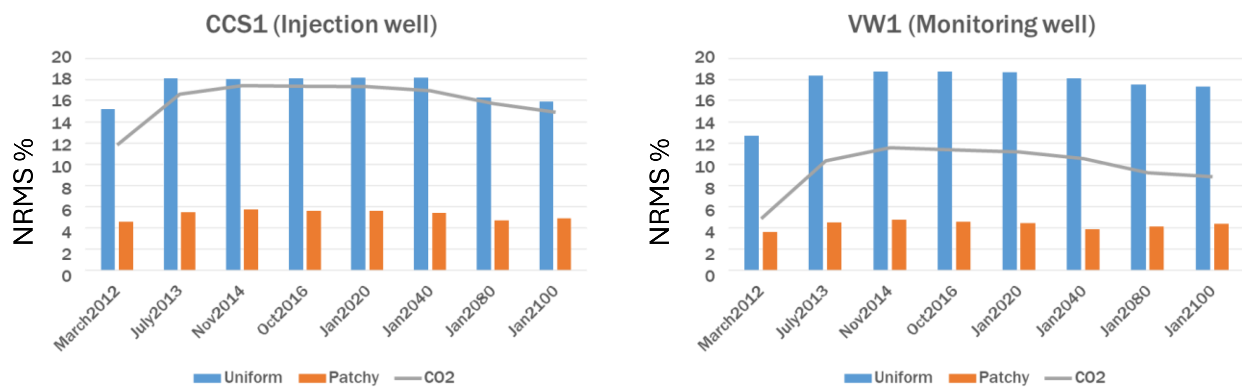


**Figure 26.** NRMS values in the injection and monitoring wells over the years under uniform and patchy mixing conditions for a hypothetical 10 Mt of $CO_2$ injection. The grey line indicates the percentage change in $CO_2$ saturation at the injection (left) and monitoring (right) wells.

Our study indicates that the time-lapse surface seismic with the survey setup similar to the one used in the study area is not highly effective and definitive in detecting $CO_2$ plume boundary, especially considering SNR in the field settings. This may not be the case everywhere, as shown in many other successful case studies of 4D seismic (for example, Sleipner project). As a part of this study, we analyzed the nominal fold of the baseline 3D seismic at the Decatur site and locations of the injection and monitoring wells (Bauer et al., 2019). Published nominal fold coverage map from Bauer et al. (2019) shows that the injection well (CCS #1) was placed mostly in the moderate-to-low nominal fold area of the 3D seismic data, which would affect the quality of characterization, modeling, and monitoring studies. As per Bauer et al. (2019), the acquisition of the 3D seismic surveys at the Decatur site presented many dynamic challenges, such as the noise generated from adjacent heavy industry and transportation infrastructure, and seasonal variation. Surface infrastructure prevented the seismic survey from obtaining adequate source and receiver points over the entire area needed for an ideal migration aperture (Coueslan et al., 2009). Some of these challenges were handled to an extent by acquiring additional data and advanced processing over time. Many of these factors can affect other onshore CCS site operations as well. Therefore, we recommend the establishment of proper baseline data and strategic placement of injection and observation wells (as per technical requirements and logistics).

We also analyzed publicly available time-lapse VSP (vertical Seismic Profile) data from the Decatur site and estimated the NRMS amplitude values for each monitor case. However, due to the significant presence of noise in the data, the NRMS amplitude values were abnormally high, leading to unreliable interpretations. We did not find a significant degree of quantitative correlation between simulated $CO_2$ plume and NRMS responses within the study area. NRMS amplitude values outside of the injection zone also indicate poor matching and cross-equalization of baseline and time-lapse data. Our investigation of the time-lapse VSP data did not reveal much insights, as these datasets had very high NRMS responses (poor repeatability) and affected by different ground conditions, resulting poor-quality of data. Finley et al. (2013) also studied one baseline VSP and first time-lapse VSP (monitor 1), which coincided with one PNC log acquisition and after when ~70,000 tonnes of $CO_2$ were already injected in the reservoir. Although Finely et al. (2013) did not find any definitive amplitude differences from these time-lapse VSP surveys that could be attributed to $CO_2$, the NRMS metric showed various interesting patterns. This included highly repeatable data (NRMS range: 9-20%) in the zones above the main injection window in the lower Mt. Simon Sandstone and high NRMS values (range: 35-65%). High NRMS values can result from low fold coverage at the depth of $CO_2$ injection, but high NRMS in some areas with good fold coverage may be suggestive of $CO_2$ plume within the Mt. Simon reservoir. A later study by Coueslan et al. (2014) with the help of three time-lapse VSP monitoring surveys confirms the degradation of the later 3D VSP imaging quality due to fewer shot points and varying ground conditions (e.g., wet, dry, damp, and frozen). Coueslan et al. (2014) still suggested that a repeatability anomaly developed in the injection interval indicative of $CO_2$ plume development over time.

The IBDP collected and provided significant and key data to the public for ongoing and future research and field deployment of CCS worldwide. Most importantly, it showed that $CO_2$ can be stored in the reservoir (as of today's knowledge). Lessons learned from such field scale demonstrations with publicly available data are crucial to advance the overall science and technology of capture and storage, societal acceptance, build team capacity, and gain experience on large-scale $CO_2$ storage. We expect such integrated projects to continue and expand their footprints in the future.

## RECOMMENDATIONS FOR FURTHER STUDIES

The study can be extended further by incorporating time-lapse geomechanical simulation for seismic modeling and conducting further sensitivity studies of seismic acquisition parameters, and $CO_2$ injection operational parameters. Li et al. (2024) conducted similar multi-physics modeling and sensitivity studies for another reservoir for hydrogen storage.

## CONCLUSIONS

The study is a product of a multi-disciplinary team effort, including geology, petrophysics, geophysics, and reservoir engineering. Proper integration and coordination among each team (and team members) should occur during the planning and field execution phases; otherwise, we may not receive the best quality and best possible characterization and monitoring data from the field to assure stakeholders about the value and integrity of the $CO_2$ injection program.

Our proposed workflow of integrating subsurface characterization, 3D static models, dynamic flow simulation models, rock physics studies, and time-lapse seismic forward models, validated with time-lapse PNC log measurements will facilitate designing more effective 4D seismic surveys in a real field setting to adequately detect $CO_2$ plume and quantify its saturation. This integrated workflow can help design effective time-lapse seismic or other geophysical surveys in advance.

Our seismic modeling results showed small changes in seismic amplitude due to 1 Mt of $CO_2$ injection, irrespective of rock physics modeling constraints. This might be due to the survey design, local site-specific geology, and operational parameters. With a hypothetical 10 Mt $CO_2$ injection, the $CO_2$ plume size becomes large, and the plume boundary can be detected by time-lapse seismic.

Accurate selection of appropriate rock physics models (patchy or uniform mixing) for the reservoir is important for feasibility, modeling, and field result verification studies.

More petrophysical measurements should be done to better characterize permeability, relative permeability, and capillary pressure to predict $CO_2$ plume distribution.

If surface 3D seismic modeling shows less sensitivity to $CO_2$ at a given site, time, and injection conditions, other surveys can be considered.

**ACKNOWLEDGEMENTS**

Authors thank the SEG Advanced Modeling Corporation (SEAM) for initial funding through a contract between the SEAM AI project and The University of Texas at Austin. We also acknowledge the sponsors of the TCCS IA and GAAC Career Development Grant at the Bureau of Economic Geology at The University of Texas at Austin for partially funding this study. Authors also thank Sergey Fomel, Dallas Dunlap, and Ben Gremillion at The University of Texas at Austin for providing project leadership, funding, and support for the initial part of the study. Special thanks to the Computer Modeling Group (CMG) for providing simulation software. Thanks to SLB and GeoActive for donating Petrel$^{TM}$ and Interactive Petrophysics$^{TM}$ software, respectively, to The University of Texas at Austin.

**DATA AVAILABILITY**

The subsurface data (well logs and seismic) used in this project can be found on the NETL-EDX program website: https://edx.netl.doe.gov/group/illinois-basin-decatur-project. The Madagascar programing codes for time-lapse rock physics and seismic modeling are provided in Appendix.

**CRediT STATEMENT**

Shuvajit Bhattacharya: Conceptualization, Methodology, Formal Analysis, Investigation, Resources, Writing - Original Draft, Visualization, Supervision, Software, Project administration, Funding acquisition; Sujith Swaminadhan: Formal Analysis, Investigation, Visualization, Validation, Data Curation, Methodology, Software; Sahar Bakhshian: Formal Analysis, Investigation, Investigation, Visualization, Validation, Data Curation, Methodology, Software, Writing - Review & Editing

## REFERENCES


Azuma, H., C. Konishi, and Z. Xue, 2013, Introduction and application of the modified patchy saturation for evaluating $CO_2$ saturation by seismic velocity: *Energy Procedia*, 37, 4024–4032.

Coueslan, M. L., Leetaru, H. E., Brice, T., Leaney, W. S., and McBride, J. H., 2009, Designing a seismic program for an industrial CCS site: Trials and 410 tribulations, Energy Procedia, 1(1), 2193–2200

Bukar, I., Bell, R.E., Muggeridge, A., and Krevor, S., 2024, Carbon dioxide migration along faults at the Illinois Basin – Decatur Project 1 revealed using time shift analysis of seismic monitoring data, https://doi.org/10.31223/X51696

Coueslan, M. L., Ali, S., Campbell, A., Nutt, W., Leaney, W., Finley, R., and Greenberg, S., 2013, Monitoring CO2 injection for carbon capture and storage using time-lapse 3D VSPs, The Leading Edge, 32 (10), 1268–1276.

Gassmann, F., 1951, Elastic waves through a packing of spheres: *Geophysics*, 16, 673–685.

IBDP, 2021, Illinois State Geological Survey (ISGS), Illinois Basin - Decatur Project (IBDP) geological models, July 7, 2021. Midwest geological sequestration consortium (MGSC) phase iii data sets. DOE cooperative agreement no. de-fc26-05nt42588., doi: 10.18141/1854141.

Illinois State Geological Survey (ISGS), Illinois Basin - Decatur Project (IBDP) CO2 Injection Monitoring Data, April 30, 2021. Midwest Geological Sequestration Consortium (MGSC) Phase III Data Sets. DOE Cooperative Agreement No. DE-FC26-05NT42588.

Ivanova, A., A. Kashubin, N. Juhojuntti, J. Kummerow, J. Henninges, C. Juhlin, S. Lu¨th, and M. Ivandic, 2012, Monitoring and volumetric estimation of injected $CO_2$ using 4D seismic, petrophysical data, core measurements and well logging: a case study at Ketzin, Germany: *Geophysical Prospecting*, 60, 957–973.

Kazemeini, S.H., Juhlin, C. and Fomel, S., 2010. Monitoring CO2 response on surface seismic data; a rock physics and seismic modeling feasibility study at the CO2 sequestration site, Ketzin, Germany. *Journal of Applied Geophysics*, *71*(4), pp.109-124.

Lumley, D., 2010, 4d seismic monitoring of $CO_2$ sequestration: *The Leading Edge*, 29, 150–155.

Mavko, G., and T. Mukerji, 1998, Bounds on low-frequency seismic velocities in partially saturated rocks: *Geophysics*, 63, 918–924.

Mavko, G., T. Mukerji, and J. Dvorkin, 2020, The rock physics handbook: Cambridge University Press.

Zaluski, W., Lee, S.-Y., 2019. 2018 IBDP/ICCS static geological model development and dynamic modelling updates, Schlumberger technical report.

Krevor, S. C., Pini, R., Zuo, L., & Benson, S. M. (2012). Relative permeability and trapping of $CO_2$ and water in sandstone rocks at reservoir conditions. Water resources research, 48(2).

Lahann, R., Rupp, J., & Medina, C. (2014). An evaluation of the seal capacity and $CO_2$ retention properties of the Eau Claire Formation (Cambrian). Environmental Geosciences, 21(3).

CMG-GEM, 2012, Advanced compositional and unconventional reservoir simulator: Computer Modeling Group Ltd.

Freiburg, J., Morse, D., Leetaru, H., Hoss, R., and Qina, Y., 2014, Depositional and diagenetic characterization of the Mt Simon Sandstone at the Illinois Basin; Decatur Project Carbon Capture and Storage Site, Decatur, Illinois, USA. Circular 583. Urbana, IL: University of Illinois at Urbana-Champaign, Institute of Natural Resource Sustainability, Illinois State Geological Survey, Urbana, IL, United States. doi:2142/55338

Greenberg, S.E., 2021, An Assessment of Geologic Carbon Sequestration Options in the Illinois Basin: Phase III, Final Report prepared for the US Department of Energy.

Zaluski, W., and Lee, S-Y., 2019, 2018 IBDP/ICCS Static Geological Model Development and Dynamic Modelling (available on https://edx.netl.doe.gov/group/illinois-basin-decatur-project)

https://edx.netl.doe.gov/group/illinois-basin-decatur-project (Accessed March 30, 2023)

Harvey, S., Hopkins, J., Kuehl, H., Simon O'Brien, S., and Mateeva, A., 2022, Quest CCS facility: Time-lapse seismic campaigns, International Journal of Greenhouse Gas Control, Volume 117 https://doi.org/10.1016/j.ijggc.2022.103665.

Li, C., Bhattacharya, S, Alhotan, M.M., Delshad, M., 2024, Time-lapse geophysical responses of hydrogen-saturated rock: Implications on subsurface monitoring, https://doi.org/10.31223/X52985

Finley, R.J., Frailey, S.M., Leetaru, H. E., Ozgur S., Marcia L. C., and Marsteller, S., 2013, Early Operational Experience at a One-million Tonne CCS Demonstration Project, Decatur, Illinois, USA, GHGT-11, Energy Procedia 37, 6149– 6155

Chadwick, R.A., Noy, D., Arts, R., and Eiken, O., 2009, Latest time-lapse seismic data from Sleipner yield new insights into CO2 plume development, Energy Procedia, Volume 1, Issue 1, February 2009, Pages 2103-2110

Zhang, R., Ghosh, R., Sen, M.K., Srinivasan, S., 2013, Time-lapse surface seismic inversion with thin bed resolution for monitoring CO2 sequestration: A case study from Cranfield, Mississippi, International Journal of Greenhouse Gas Control, Volume 18, October 2013, Pages 430-438

Wang, Z., Harbert, W.P., Dilmore, R.M., Huang, L., 2018, Modeling of time-lapse seismic monitoring using CO2 leakage simulations for a model CO2 storage site with realistic geology: Application in assessment of early leak-detection capabilities, International Journal of Greenhouse Gas Control, Volume 76, September 2018, Pages 39-52

Arts, R. J., M. Trani, R. A. Chadwick, O. Eiken, S. Dortland, and L. G. H. van der Meer, 2009, Acoustic and elastic modeling of seismic time-lapse data from the Sleipner CO2 storage operation, in M. Grobe, J. C. Pashin, and R. L. Dodge, eds., Carbon dioxide sequestration in geological media—State of the science: AAPG Studies in Geology 59, p. 391–403. DOI:10.1306/13171251St593387Arts et al. (2009)

Ajo-Franklin, J.B., Peterson, J., Doetsch, J., and Daley, T.M., 2013, High-resolution characterization of a CO2 plume using crosswell seismic tomography: Cranfield, MS, USA, International Journal of Greenhouse Gas Control, Volume 18, October 2013, Pages 497-509

Bergmann, P., Schmidt-Hattenberger, C., Kiessling, D., Rücker, C., Labitzke, T., Henninges, J., Baumann, G., and Schütt, H., 2012, Surface-downhole electrical resistivity tomography applied to monitoring of CO2 storage at Ketzin, Germany, GEOPHYSICS 77: B253-B267. https://doi.org/10.1190/geo2011-0515.1

Mawalkar, S., Brock, D., Burchwell, A., Kelley, M., Mishra, S., Gupta, N., Pardini, R., and Shroyer, B., 2019, Where is that CO2 flowing? Using Distributed Temperature Sensing (DTS) technology for monitoring injection of CO2 into a depleted oil reservoir, International Journal of Greenhouse Gas Control, Volume 85, Pages 132-142, https://doi.org/10.1016/j.ijggc.2019.04.005

Bhakta, T., Paap, B., Vandeweijer, V., and Trond M., 2022, Monitoring of CO2 plume movement using time-lapse distributed acoustic sensing (DAS) data, Paper presented at the SEG/AAPG International Meeting for Applied Geoscience & Energy, Houston, Texas, USA, https://doi.org/10.1190/image2022-3745759.1

Yao, C., Chen, H., Onishi, T., Datta-Gupta, A., Mishra, S., Mawalkar, S., and Pasumarti, A., 2024, Robust CO2 plume imaging by joint tomographic inversion using distributed pressure and temperature measurements, International Journal of Greenhouse Gas Control, Volume 135, https://doi.org/10.1016/j.ijggc.2024.104166.

Gasperikova, E., Appriou, D., Bonneville, A., Feng, Z., Huang, L., Gao, K., Yang, X., and Daley, T., 2024, Sensitivity of geophysical techniques for monitoring secondary CO2 storage plumes,

International Journal of Greenhouse Gas Control, Volume 114, https://doi.org/10.1016/j.ijggc.2022.103585

Bhattacharya. S., Swaminadhan, S., and Bakhshian, S., 2024, Building Realistic Time-Lapse Seismic Models for CO2 Plume Monitoring, Integrating Geology, Reservoir Simulation, and Rock Physics: Case Study from an Onshore CCS Site, United States, presented at SEG Geophysical Research for Gigatonnes CO2 Storage workshop, Golden, Colorado

Kazemeini, S.H., Juhlin, C., and Fomel, S., 2010, Monitoring CO2 response on surface seismic data; a rock physics and seismic modeling feasibility study at the CO2 sequestration site, Ketzin, Germany, Journal of Applied Geophysics, Volume 71, Issue 4, Pages 109-124.

Fomel, S., 2002, Applications of plane-wave destruction filters: Geophysics, v. 67, 1946-1960.

Fomel, S., 2010, Predictive painting of 3D seismic volumes, GEOPHYSICS 75: A25-A30.

https://doi.org/10.1190/1.3453847

Fomel, S., 2016, Fast scattered data gridding: 86th Annual International Meeting, SEG, 4059-4063.

Shoemaker, M., Narasimhan, S., Quimby, S., and Hawkins, J., 2019, Calculating far-field anisotropic stress from 3D seismic in the Permian Basin. The Leading Edge, 38 (2): 96–105. doi: https://doi.org/10.1190/tle38020096.1

Bauer RA, Will R, E. Greenberg S, Whittaker SG. Illinois Basin–Decatur Project. In: Davis TL, Landrø M, Wilson M, eds. Geophysics and Geosequestration. Cambridge University Press; 2019:339-370.

Van Genuchten, M. T., 1980, A closed-form equation for predicting the hydraulic conductivity of unsaturated soils. Soil Science Society of America journal, 44(5), 892-898.

CMG, G., 2021, Advanced compositional and unconventional reservoir simulator Version 2021. CMG Ltd., CM Group, Editor.

Bakhshian, S., Bump, A. P., Pandey, S., Ni, H., and Hovorka, S. D., 2023, Assessing the potential of composite confining systems for secure and long-term CO2 retention in geosequestration. Scientific Reports, 13(1), 21022.

## APPENDIX

**The detailed workflow for time-lapse seismic modeling**

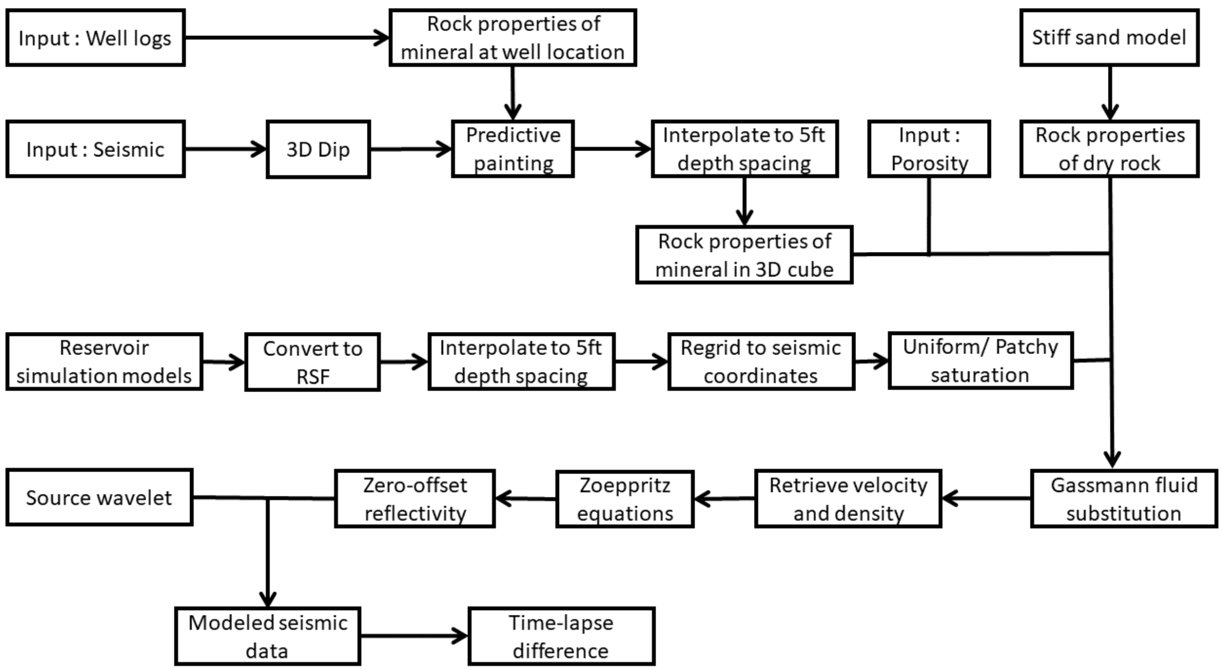


**Programing codes**

**Time-lapse rock physics and seismic modeling**

```
from rsf.proj import *
import math

## ----------------------------------------------
## Input data
## SEGYs - ../../inputs/IBDP_Seismic/data/IBDP_3D_Seismic_Volume_Reprocessed/Depth-PSTM/
## CO2 simulation - ../../inputs/Gas-Saturation/1Mt/
## Well data - ../../inputs/well_data/
## ----------------------------------------------


## Read SEGY data

```

```
path  =  '../../inputs/IBDP_Seismic/data/IBDP_3D_Seismic_Volume_Reprocessed/Depth-PSTM/' #SEGY path

# Dictionary with SEGY file names
# loading the entire seismic data
segy = dict(impedance = path+'Acoustic-Impedance-Depth.sgy',
            porosity = path+'Porosity-NN-Depth.sgy',
            seismic = path+'pstm-Phase-Shifted-Depth.sgy')

for case in segy.keys(): # for loop to read each SEGY file

   # SEGY to RSF
   Flow([case,case+'_hdr',case+'_hdr.asc',case+'_hdr.bin'],segy[case],
      '''
      segyread tfile=${TARGETS[1]} hfile=${TARGETS[2]} bfile=${TARGETS[3]}
      ''')

   # sort 3D seismic data into inline and crossline to make a 3D volume
   if case == "seismic":
      Flow([case+'_cube',case+'_mask',case+'_map'],case,
                  '''
         intbin xk=cdpt yk=ep mask=${TARGETS[1]} map=${TARGETS[2]} |
         put label2=Crossline label3=Inline |
         window max1=8 f2=387 n3=195
         ''')
   # sort 3D impedance and porosity data into inline and crossline
   else:
      Flow([case+'_cube',case+'_mask',case+'_map'],case,
                  '''
```

```
                    intbin xk=cdpt yk=ep mask=${TARGETS[1]} map=${TARGETS[2]} |
          window max1=8 |
          put label2=Crossline label3=Inline
             ''')

# Plot seismic cube
# The window (subcube) is selected such that we plot the volume of interest
# meaning, the ploting is a zoomed version of where the CO2 is injected
Result('seismic','seismic_cube',
  '''
  window min1=5.5 max1=7.14 min2=500 n2=1450 n3=195 |
  spline o1=5.5 d1=.005 n1=328 |
  byte gainpanel=all bar=trash11.rsf |
  grey3 title="Seismic data" flat=n frame1=225
  frame2=473 frame3=83 point1=.75 point2=0.75
  scalebar=y barlabel=Amplitude color=i
  label1=Time unit1=s minval=-.12 maxval=.12
  labelsz=10 titlefat=5 labelfat=4  label1=Depth unit1=kft
  ''')

# Plot porosity cube
Result('porosity','porosity_cube',
  '''
  window min1=4.5 min2=1500 n2=1450 n3=195 | clip2 lower=0 |
  byte gainpanel=all bar=trash12.rsf mean=1 allpos=0 |
  grey3 title="Porosity" flat=n frame1=225
  frame2=10000 frame3=1 point1=.75 point2=0.75
  scalebar=y barlabel=Porosity color=j
```

```
  label1=Time unit1=s
  labelsz=10 titlefat=5 labelfat=4  label1=Depth unit1=kft
  ''')

# well data

well_path = '../../inputs/well_data/' # well data path

# Dictionary with well data details
# N - Northing, E - Easting, color - color for plotting, iltloc - inline trace location, xltloc - crossline trace location, il - inline, xl - crossline

wells = {'ccs1': {'N': 1169544.631, 'E': 342828.247, 'color': 1, 'iltloc': 176404, 'xltloc': 76649, 'il': 84, 'xl': 973},
         'vw1':  {'N': 1170573.109, 'E': 342843.594, 'color': 2, 'iltloc': 176404, 'xltloc': 115388, 'il': 84, 'xl': 1179},
         'ccs2': {'N': 1172887.910, 'E': 344366.370, 'color': 3, 'iltloc': 277406, 'xltloc': 205073, 'il': 123, 'xl': 1642},
         'vw2':  {'N': 1175108.829, 'E': 343129.865, 'color': 4, 'iltloc': 198449, 'xltloc': 291770, 'il': 92, 'xl': 2086}
         }

# Dictionary with elastic moduli for different materials
# K - Bulk modulus, mu - Shear modulus, rho - Density
# moduli values in GPa
# density values in g/cm3

moduli = {'Quartz':   {'K': 36.6  ,  'mu': 45,   'rho': 2.65},
          'Feldspar': {'K': 75.5,  'mu': 25.6,   'rho': 2.62},
          'Dolomite': {'K': 76.4,  'mu': 49.7, 'rho': 2.87},
```

```
        'Clay':    {'K': 21,    'mu': 7,    'rho': 2.55},
        'Brine':   {'K': 2.3 ,  'mu': 0,    'rho': 1.23},
        'CO2':     {'K': 0.083299, 'mu': 0,    'rho': 0.17427}
        }

# Convert bulk and shear moduli from GPa to (g/cm^3)*(ft/s)^2 for consistency
for m in moduli:
        moduli[m]['K'] *= 1e9/92.903
        moduli[m]['mu'] *= 1e9/92.903

# Dictionary with well data file names

logs = dict(ccs1 = well_path+'CCS1-Logs-Edited.las',
        ccs2 = well_path+'CCS2-Logs-Edited.las',
        vw1 = well_path+'VW1-Logs-Edited.las',
        vw2 = well_path+'VW2-Logs-Edited.las'
)


## Predictive Painting
## [ Fomel, S. (2010). Predictive painting of 3D seismic volumes. Geophysics, 75(4), A25-A30.  ]
# Dip estimation for predictive painting

# mask for zero padding
Flow('mask','seismic_cube',
   '''
   math output=0 | math output=1 |
   cut max1=5.5 |
```

```
    cut min1=7.14 |
    pad beg1=25 end1=25 |
    patch p=1,4,1
    ''')

# patch seismic cube for dip estimation
# Patching is done to make a hypercube and estimate the dips in small cubes.
# The estimated dip information in the hypercube is mapped back to original
# dimension by unpatching (or inverse patching)
Flow('patch',['seismic_cube', 'mask'],
     '''
     pad beg1=25 end1=25 |
     patch p=1,4,1
          ''')
# estimate dip in patched domain
Flow('dip_patch','patch mask','fdip mask=${SOURCES[1]} rect1=10 rect2=61 rect3=15',split=[5,'omp'])
# extract dip inline and crossline
# the estimated dip will be in 2 directions one for inline and one for crossline
Flow('dip_xl','dip_patch','window n4=1 squeeze=n | transp plane=56 | patch inv=y weight=y dim=3')
Flow('dip_il','dip_patch','window f4=1 squeeze=n | transp plane=56 | patch inv=y weight=y dim=3')
#merge inline and crossline dip components
Flow('dip','dip_xl dip_il','cat axis=4 ${SOURCES[1]}')

# 2 dip components corresponding to inline and crossline
# ( same as dip_il and dip_xl, but transposed appropriately for future usage)
Flow('dip1','dip','window n4=1 squeeze=n')
Flow('dip2','dip','window f4=1 squeeze=n | transp plane=23')
```

```

# generate ascii file with well locations
# The well locations are in the python dictionary and for further
# calculations it needs to be in file so we generate ascii file
# then convert to rsf file
Flow('xy.asc',None,
        f'''
        echo
        {wells['ccs1']['xl']-411} {wells['ccs1']['il']-2}
        {wells['ccs2']['xl']-411} {wells['ccs2']['il']-2}
        {wells['vw1']['xl']-411} {wells['vw1']['il']-2}
        {wells['vw2']['xl']-411} {wells['vw2']['il']-2}
        n1=2 n2=4 data_format=ascii_int
        in=$TARGET
        ''')
# convert ascii to RSF
Flow('xy','xy.asc','dd form=native')

# convert well locations to seismic coordinates (inline, crossline)
Flow('x2','xy','window n1=1 squeeze=n | add add=411')
Flow('y2','xy','window f1=1 squeeze=n | add add=2')
Flow('xy2','x2 y2','cat axis=1 ${SOURCES[1]}')
Flow('coord','xy2','dd type=float')

# pseudo velocity file to estimate distance map
Flow('vel','seismic_cube','window n1=1 | math output=1')
# the file coord is estimated in a coarse grid and dist is estimated in a fine grid
# using nearest neighbor interpolation
```

```
Flow('dist','coord vel','nnint coord=${SOURCES[0]} velocity=${SOURCES[1]} dist=y')

# interpolate distance map to get 4 distance maps for each wells
for i in range(4):
   Flow('coord'+str(i),'coord','window n2=1 f2=%d' % i)

   Flow('dist'+str(i),['coord'+str(i), 'vel'],'nnint coord=${SOURCES[0]} velocity=${SOURCES[1]} dist=y | scale dcscale=2')

## Read Log data and convert to RSF

for log in logs:
   Flow(log,logs[log],'las2rsf $SOURCE $TARGET')

# Dictionary with with log parameters and keys

curves = dict(dtc = 'DTCO',
   dts = 'DTSM',
   phi = 'PHIT',
   quartz = 'QUARTZ',
   dolo = 'DOLOMITE',
   kspar = 'KFELDSPAR',
   clay = 'CHLORITE+ILLITE+KAOLINITE'
   )

#extract logs for each well
# the estracted log is between 5040 ft and 7160 ft
# this is selected because of that all logs from all wells
# have non-zero values in this range
```

```
for log in logs.keys():
    for curve in curves.keys():
        Flow(log+'_'+curve,log,
                      f'''
                      headermath output={curves[curve]} segy=n |
                      window | clip2 lower=0 | window min1=5040 max1=7160
                      put label1=Depth unit1=ft o2={wells[log]['xl']}
            o3={wells[log]['il']} d2=1 d3=1 n3=1
                      ''')

# rename keys
curves['rho'] = 'Density'
curves['phi'] = 'Porosity'
curves['quartz'] = 'Quartz'
curves['kspar'] = 'K Feldspar'
curves['dolo'] = 'Dolomite'
curves['clay'] = 'Clay'

## Mineral moduli calculation

for log in logs.keys():
    ##########################################################
    #### VOIGHT-AVERAGED MODULI & DENSITY ################
    ##########################################################
    # Bulk modulus
    Flow(log+'_Kv',[log+'_quartz',log+'_kspar',log+'_dolo',log+'_clay'],
        '''
        math Q=${SOURCES[0]} K=${SOURCES[1]} D=${SOURCES[2]} C=${SOURCES[3]}
```

```
    output="(Q*%f+K*%f+D*%f+C*%f)/(Q+K+D+C+.001)"
    ''' % (moduli['Quartz']['K'],moduli['Feldspar']['K'],moduli['Dolomite']['K'],moduli['Clay']['K']))
  # Shear modulus
  Flow(log+'_muv',[log+'_quartz',log+'_kspar',log+'_dolo',log+'_clay'],
    '''
    math Q=${SOURCES[0]} K=${SOURCES[1]} D=${SOURCES[2]} C=${SOURCES[3]}
    output="(Q*%f+K*%f+D*%f+C*%f)/(Q+K+D+C+.001)"
    ''' % (moduli['Quartz']['mu'],moduli['Feldspar']['mu'],moduli['Dolomite']['K'],moduli['Clay']['mu']))
  # Density
  Flow(log+'_rho_min',[log+'_quartz',log+'_kspar',log+'_dolo',log+'_clay'],
    '''
    math Q=${SOURCES[0]} K=${SOURCES[1]} D=${SOURCES[2]} C=${SOURCES[3]}
    output="(Q*%f+K*%f+D*%f+C*%f)/(Q+K+D+C+.001)"
    ''' % (moduli['Quartz']['rho'],moduli['Feldspar']['rho'],moduli['Dolomite']['rho'],moduli['Clay']['rho']))

  ####################################################
  #### REUSS-AVERAGED MODULI  ########################
  ####################################################
  # Bulk modulus
  Flow(log+'_Kr',[log+'_quartz',log+'_kspar',log+'_dolo',log+'_clay'],
    '''
    math Q=${SOURCES[0]} K=${SOURCES[1]} D=${SOURCES[2]} C=${SOURCES[3]}
    output="(Q+K+D+C)/(Q*%f+K*%f+D*%f+C*%f+.001)"
    ''' % (moduli['Quartz']['K'],moduli['Feldspar']['K'],moduli['Dolomite']['K'],moduli['Clay']['K']))
  # Shear modulus
  Flow(log+'_mur',[log+'_quartz',log+'_kspar',log+'_dolo',log+'_clay'],
    '''
```

```
    math Q=${SOURCES[0]} K=${SOURCES[1]} D=${SOURCES[2]} C=${SOURCES[3]}
    output="(Q+K+D+C)/(Q*%f+K*%f+D*%f+C*%f+.001)"
    '''                                                                      %
(moduli['Quartz']['mu'],moduli['Feldspar']['mu'],moduli['Dolomite']['K'],moduli['Clay']['mu']))

  ###########################################################################
  #### REUSS-VOIGHT-HILL AVERAGED MODULI for mineral matrix  #############
  ###########################################################################
  # Bulk modulus
  Flow(log+'_K_min',[log+'_Kr',log+'_Kv'],
  '''
  math Kr=${SOURCES[0]} Kv=${SOURCES[1]}
  output="(Kr+Kv)/2"
  ''')
  # Shear modulus
  Flow(log+'_mu_min',[log+'_mur',log+'_muv'],
  '''
  math Kr=${SOURCES[0]} Kv=${SOURCES[1]}
  output="(Kr+Kv)/2"
  ''')

        # resample and filter logs (Bulk and Shear moduli, Density, Porosity)
  # the sampling of well logs are 0.5 ft and seismic is 5 ft
  # the need for resampling is to match the sampling of both
  # essentially the logs are resampled to 5 ft
  for curve in ['K_min','mu_min','rho_min','phi']:
    Flow(log+'_'+curve+'_filt',log+'_'+curve,
      '''
      window min1=5500 max1=7140 |
```

```
      pad2 top=500 bottom=500 |
      bandpass fhi=.025 | window min1=5500 max1=7140 |
      window j1=40 |
      pad2 top=300 bottom=68 |
      put d1=.02 o1=-.5
      ''')
tmp = ['vp','vs']
i = 0
# resample and filter logs (Vp, Vs)
for curve in ['dtc','dts']:
   Flow(log+'_'+curve+'_filt',log+'_'+curve,
      '''
      window min1=5500 max1=7140 |
      pad2 top=500 bottom=500 |
      bandpass fhi=.025 | window min1=5500 max1=7140 |
      window j1=40 |
      pad2 top=300 bottom=68 |
      put d1=.02 o1=-.5
      ''')
   Flow(log+'_'+tmp[i]+'_filt',log+'_'+curve+'_filt','math output="10^6/input"')
   i += 1

# Vp/Vs ratio
Flow(log+'_vpvsr_filt',[log+'_dtc_filt', log+'_dts_filt'],
   '''
   math num=${SOURCES[1]} den=${SOURCES[0]}
   output="num/den"
   ''')
```

```
################################################################################
```

**Predictive painting**

```
################################################################################
# penalty function for painting
# F(x) = exp(rms(x_i)) where x_i is trace at location x and rms() is the root mean square of the trace
Flow('wcost1','dip_il','stack axis=1 rms=y norm=n | math output="exp(input)" ')
Flow('wcost2','dip_xl','stack axis=1 rms=y norm=n | math output="exp(input)" ')
Flow('wcost','wcost1 wcost2','cat axis=3 ${SOURCES[1]} | smooth rect1=40 rect2=40')

# loop over wells
for well in wells.keys():
    Flow(well+'-wtime2','wcost',
        '''
        mul $SOURCE | stack axis=3 norm=n |
        put o1=0 d1=1 o2=0 d2=1 o3=0 d3=1 |
        eikonal vel=n zshot=%d yshot=%d
        ''' % (wells[well]['xl'],wells[well]['il']))

# loop over logs for painting
i = 0
for log in logs.keys():
    for curve in ['K_min','mu_min','rho_min','vpvsr','vp','vs']:
        source = log + '_' + curve + '_filt'
        Flow(log+'_'+curve+'_paint',['dip', source, 'dist'+str(i)],
            '''
            pwpaint2 seed=${SOURCES[1]} cost=${SOURCES[2]} order=3
            ''')
```

```
    i += 1

# mean of painted logs from each wells (looped over logs)
for curve in ['K_min','mu_min','rho_min','vpvsr','vp','vs']:
    Flow(curve+'_paint_mean',[log+'_'+curve+'_paint' for log in logs.keys()],
        '''
        cat ${SOURCES[1:4]} axis=4 | stack axis=4 | window f1=25 n1=401 | spline n1=1601 d1=.005
o1=0
        ''')

sufx = "_paint_mean" # suffix for painted logs

# interpolate painted logs to seismic coordinates
for curve in ['K_min','mu_min','rho_min','vpvsr']:
    Flow(curve,[curve+sufx],'spline n1=1601 d1=.005 o1=0')

# interpolate painted Vp, Vs logs to seismic coordinates
for curve in ['vp','vs']:
    Flow(curve+'_true',[curve+sufx],'spline n1=1601 d1=.005 o1=0')

# plot mineral density
Plot('rho_min','rho_min',
    '''
    window min1=4.5 min2=700 max2=1200 min3=50 max3=120|
    byte gainpanel=all bar=trash1.rsf mean=y |
    grey3 title="Density" flat=n color=j
    frame1=0 frame2=500 frame3=0 point1=0.75 point2=0.75
    scalebar=y
    label1=Depth unit1=kft
```

```
    ''')
# plot mineral bulk modulus
Plot('K_min','K_min',
    '''
    window min1=4.5 min2=700 max2=1200 min3=50 max3=120|
    byte gainpanel=all bar=trash2.rsf mean=y |
    grey3 title="Bulk Modulus" flat=n color=j
    frame1=0 frame2=500 frame3=0 point1=0.75 point2=0.75
    scalebar=y
    label1=Depth unit1=kft
    ''')
# plot mineral shear modulus
Plot('mu_min','mu_min',
    '''
    window min1=4.5 min2=700 max2=1200 min3=50 max3=120|
    byte gainpanel=all bar=trash3.rsf mean=y |
    grey3 title="Shear Modulus" flat=n color=j
    frame1=0 frame2=500 frame3=0 point1=0.75 point2=0.75
    scalebar=y
    label1=Depth unit1=kft
    ''')
# plot Vp/Vs ratio
Plot('vpvsr','vpvsr',
    '''
    window min1=4.5 min2=700 max2=1200 min3=50 max3=120|
    byte gainpanel=all bar=trash4.rsf mean=y |
    grey3 title="Vp/Vs Ratio" flat=n color=j
    frame1=0 frame2=500 frame3=0 point1=0.75 point2=0.75
```

```
   scalebar=y
   label1=Depth unit1=kft
   ''')
# Plot all figures in 1 file
Result('min_matrix','K_min mu_min rho_min vpvsr','TwoColumns')

# interpolate porosity cube (from the inversion) to seismic coordinates
Flow('phi','porosity_cube.rsf',
   '''
   dd type=float |
   spline n1=1601 d1=.005 o1=0 |
   clip2 lower=0
   ''')

# Bulk density
Flow('rho','phi rho_min',
   '''
   math phi=${SOURCES[0]} rho=${SOURCES[1]}
   output="phi*%f+(1-phi)*rho"
   '''% moduli['Brine']['rho'])

## Hertz-Mindlin (HM) model

g = 32.17 #acceleration due to gravity in ft/s^2
c = 6       # coordination number
phi_c = .4  # critical porosity

Flow('p_eff','rho',
```

```
    '''
    math rho=$SOURCE
    output="(rho-%f)*%f*5" |
    causint
    ''' % (moduli['Brine']['rho'],g))

Flow('poisson','vpvsr',
    '''
    math r=$SOURCE
    output="(r^2 - 2) / (2*r^2 - 2)"
    ''')

# HM Bulk modulus
Flow('K_hm',['mu_min','p_eff','poisson'],
    '''
    math mu=${SOURCES[0]} peff=${SOURCES[1]} nu=${SOURCES[2]}
    output="(%d^2*(1-%f)^2*mu^2/(18*%f^2*(1-nu)^2)*peff)^(1/3)"
    ''' % (c,phi_c,math.pi))
# HM Shear modulus
Flow('mu_hm','mu_min p_eff poisson',
     '''
     math mu=${SOURCES[0]} peff=${SOURCES[1]} nu=${SOURCES[2]}
     output="(5-4*nu)/(5*(2-nu))*(3*%d^2*(1-%f)^2*mu^2/(2*%f^2*(1-nu)^2)*peff)^(1/3)"
     ''' % (c,phi_c,math.pi))


####################################################################################
Stiff-sand Model
```

```
##################################################################################

# StiffSand model for bulk modulus
# estimated for the entire cube
Flow('K_stiff',['phi', 'K_hm', 'mu_min', 'K_min'],
    '''
    math phi=${SOURCES[0]} khm=${SOURCES[1]}
    mhm=${SOURCES[2]} km=${SOURCES[3]}
    output="((phi/%f)/(khm+(4/3)*mhm)+(1-phi/%f)/(km+(4/3)*mhm))^(-1)-(4/3)*mhm"
    ''' % (phi_c, phi_c))

# StiffSand model for shear modulus
Flow('z_hm','K_min mu_min',
    '''
    math kh=${SOURCES[0]} mh=${SOURCES[1]}
    output="(mh/6)*((9*kh+8*mh)/(kh+2*mh))"
    ''')

Flow('mu_stiff',['phi','z_hm', 'mu_hm', 'mu_min'],
    '''
    math phi=${SOURCES[0]} zhm=${SOURCES[1]}
    mhm=${SOURCES[2]} mm=${SOURCES[3]}
    output="((phi/%f)/(mhm+zhm)+(1-phi/%f)/(mm+zhm))^(-1)-zhm"
    ''' % (phi_c, phi_c))

##################################################################################
Gassmann Fluid Substitution
##################################################################################
```

```
## This calculations are for the entire volume
## Insitu case - 100% brine

# Bulk modulus for 100% brine
Flow('K_sat_w',['K_stiff', 'K_min', 'phi'],
   '''
   math kd=${SOURCES[0]} km=${SOURCES[1]} phi=${SOURCES[2]}
   output="kd+((1-kd/km)^2/(phi/%f+(1-phi)/km-kd/km^2+1e-10))"
   ''' % (moduli['Brine']['K']))

# Vp for 100% brine
Flow('vp','K_sat_w mu_stiff rho',
   '''
   math ks=${SOURCES[0]} mu=${SOURCES[1]} rho=${SOURCES[2]}
   output="sqrt((ks+4/3*mu)/rho)"
   ''')

# Acoustic impedance for 100% brine
Flow('ai','vp rho','mul ${SOURCES[1]}')

# Plot Vp and AI for 100% brine as baseline
Result('vp_baseline','vp',
   '''
   window min1=4.5 min2=800 max2=1300 min3=50 max3=120|
   byte gainpanel=all bar=trash5.rsf mean=y |
   grey3 title="Baseline Vp" flat=n color=j
   frame1=0 frame2=500 frame3=0 point1=0.75 point2=0.75
   scalebar=y
```

```
   label1=Depth unit1=kft
   ''')

Result('ai_baseline','ai',
   '''
   window min1=4.5 min2=800 max2=1300 min3=50 max3=120|
   byte gainpanel=all bar=trash6.rsf mean=y |
   grey3 title="Baseline AI" flat=n color=j
   frame1=0 frame2=500 frame3=0 point1=0.75 point2=0.75
   scalebar=y
   label1=Depth unit1=kft
   ''')

# convert acoustic impedance to zero-offset reflectivity

nt = 651 # number of time samples for depth to time conversion
# estimate reflectivity
Flow('refl','ai vp',
   '''
   ai2refl | put d1=5 unit1=ft |
   depth2time velocity=${SOURCES[1]}
   nt=%d dt=.002 t0=0
   '''% nt)

## Define Klauder wavelet for convolution modeling
fl = 5 # low frequency
fh = 55 # high frequency
T = 6 # wavelet length in time
```

```
k = (fh-fl) / T # wavelet slope
f0 = .5 * (fh+fl) # wavelet center frequency

# compare amplitude spectrum of segy data and generated wavelet
# spectra from segy data
Flow('seismic_spectra','seismic_cube vp',
    '''
    spline n1=1601 d1=.005 o1=0 | put d1=5 unit1=ft |
    depth2time velocity=${SOURCES[1]} nt=%d dt=.002 t0=0 |
    pad2 top=225 bottom=225 | normalize type=s |
    spectra all=y
    ''' % nt)
# spectra from reflectivity
Flow('refl_spectra','refl','pad2 top=225 bottom=225 | normalize type=s |spectra all=y')
# spectra for wavelet in segy
Flow('spectra','seismic_spectra refl_spectra','divn den=${SOURCES[1]} rect1=3')

# defined Klauder wavelet
Flow('wavelet',None,
   '''
   math type=complex
   n1=1101 d1=0.002 o1=-1.101
   output="sin(%f*%f*x1*(%f-x1))/(%f*%f*x1*exp(2*%f*I*%f*x1))" |
   real |
   spline n1=1101 d1=0.002 o1=-1.1 | normalize type=s
   ''' % (math.pi,k,T,math.pi,k,math.pi,f0))
# spectra for wavelet
Flow('wavelet_spectra','wavelet','spectra all=y')
```

```
# plot spectra for both wavelets
Result('spectra','spectra wavelet_spectra','cat axis=2 ${SOURCES[1]} | graph dash=10 title="Spectra" label1=Frequency unit1=Hz label2= unit2=')

################################################################################
```

**Baseline Seismic**

```
################################################################################

# Even though the baseline 3D surface seismic data is generated in the IBDP project dataset
# we generate the baseline seismic data for the entire volume
# This is because if we use the baseline seismic data from the dataset and we estimate the time-lapse difference for the generated seismic data for different gas saturation, the time-lapse difference gives non-zero values for the entire volume, which should not be the case. To rectify this, we generate the baseline seismic data for the entire volume

# baseline seismic data from convolving reflectivity with wavelet
Flow('baseline','refl wavelet.rsf',
     '''
     convft other=${SOURCES[1]} |
     window f1=550 n1=%d |
     put unit1=s
     '''% nt)

# Vp in kft/s for converting time to depth
Flow('vp_kft','vp','add scale=.001')
# convert baseline from time to depth
Flow('baseline_depth','baseline vp_kft','time2depth velocity=${SOURCES[1]} | put unit1=kft')
```

**# Plot baseline seismic data**

```
Result('baseline','baseline_depth',
```

```
    '''
    window min1=5.5 max1=7.14 min2=500 n2=1450 n3=195 |
    byte gainpanel=all bar=trash7.rsf |
    grey3 title="Generated Seismic data" flat=n frame1=225
    frame2=473 frame3=83 point1=.75 point2=0.75
    scalebar=y barlabel=Amplitude color=i
    label1=Time unit1=s minval=-.12 maxval=.12
    labelsz=10 titlefat=5 labelfat=4  label1=Depth unit1=kft
    ''')

# Movie for compare generated baseline and original seismic data
Plot('baseline','Fig/baseline.vpl Fig/seismic.vpl','Movie',view=1)

## Export to segy data

# Create header keys
# inline keys from impedance header
Flow('xline-mask','impedance_hdr',
     '''
     headermath output=tracr | mask min=410 n=2970 | window
     ''')
# crossline keys from impedance header
Flow('iline-mask','impedance_hdr xline-mask',
     '''
     headerwindow mask=${SOURCES[1]} |
     headermath output=ep | mask min=1 | window
     ''')
# impedance header keys
```

```
Flow('wtimpedance','impedance_hdr xline-mask iline-mask',
    '''
    headerwindow mask=${SOURCES[1]} |
    headerwindow mask=${SOURCES[2]}
    ''')
# impedance header keys for 3D
Flow('wtimpedance-3d wtimpedance-map','wtimpedance',
    '''
    intbin head=$SOURCE map=${TARGETS[1]}
    xk=tracr yk=ep
    ''')

# crossline keys
Flow('xline','baseline','window n1=1 | math output=x1 | dd type=int')
# inline keys
Flow('iline','baseline','window n1=1 | math output=x2 | dd type=int')
# source x keys
Flow('sx','wtimpedance-3d','headermath output=sx | window')
# source y keys
Flow('sy','wtimpedance-3d','headermath output=sy | window')
# depth interval key
Flow('dz','sy','dd type=float | math output=5 | dd type=int')
# time interval key
Flow('dt','sy','dd type=float | math output=2000 | dd type=int')
# header keys for depth files
Flow('zheader','baseline_depth xline iline sx sy dz',
    '''
    segyheader xline=${SOURCES[1]} iline=${SOURCES[2]}
```

```
    sx=${SOURCES[3]} sy=${SOURCES[4]}
    dt=${SOURCES[5]}
    ''')
# header keys for time files
Flow('theader','baseline xline iline sx sy dt',
    '''
    segyheader xline=${SOURCES[1]} iline=${SOURCES[2]}
    sx=${SOURCES[3]} sy=${SOURCES[4]}
    dt=${SOURCES[5]}
    ''')

# write baseline data into directory "SEGYs"
Flow('./SEGYs/baseline.sgy','baseline theader','segywrite tfile=${SOURCES[1]}')
# test exported file
Flow('test_baseline test_baseline_hdr', 'SEGYs/baseline.sgy', 'segyread tfile=${TARGETS[1]} yerb=y')
# write porosity data into directory "SEGYs"
Flow('./SEGYs/porosity.sgy','phi zheader','segywrite tfile=${SOURCES[1]}')

#####################################################################################
Reading the Simulation Files
#####################################################################################

DATAPATH = "../../inputs/Gas-Saturation/1Mt/" # data path for gas saturation files

# array of gas saturation file names
files = ["Gas_Saturation_March2012.txt", "Gas_Saturation_July2013.txt", "Gas_Saturation_Nov2014.txt", "Gas_Saturation_Oct2016.txt", "Gas_Saturation_Jan2020.txt", "Gas_Saturation_Jan2040.txt", "Gas_Saturation_Jan2080.txt", "Gas_Saturation_Jan2100.txt"]

```

```
# read gas saturation files
# a phthon script is used to read the files (read_file.py)
for file in files:
    tmp = file[15:-4]+'.rsf'
    Flow(tmp, DATAPATH+file, './read_file.py inp=$SOURCE')


# read grid coordinates
Flow('X',DATAPATH+'Grid-Centroid-X.txt','./read_file.py inp=$SOURCE') # read x coordinates
Flow('Y',DATAPATH+'Grid-Centroid-Y.txt','./read_file.py inp=$SOURCE') # read y coordinates
Flow('Z',DATAPATH+'Grid-Z.txt','./read_file.py inp=$SOURCE') # read z coordinates

# The gas saturation file is generated using CMG with an irregular grid
# Since Madagascar deals with regular grid, we interpolate and regrid the gas saturation files
# to the synthetic seismic coordinates

# extract single z plane
Flow('z-grid','Z','transp plane=13')
# extract single x plane
Flow('x-grid','X',
    '''
    window n3=1 | spray axis=3 n=100
    ''')
# extract single y plane
Flow('y-grid','Y',
    '''
    transp |
    window n3=1 | spray axis=3 n=100
```

```
  ''')
# combine x and y planes
Flow('grid','x-grid y-grid','transp | cat ${SOURCES[1]} axis=4 | transp plane=34 | transp')

### Interpolate the gas saturation cubes into seismic geometry

pco2, pco22 = [], [] # empty arrays for 3D plots
ccs1, vw1 = [], [] # empty arrays for saturation plots
i = 0 # index for year
year = ['2012', '2013', '2014', '2016', '2020', '2040', '2080', "2100"] # years for simulation files

# loop over simulation files
for file in files:
  tmp = file[15:-4] # extract year and month from file name

  # interpolate gas saturation files in z direction
  Flow(tmp+'-int1',tmp+' z-grid',
    '''
                cut n3=20 f3=0 | cut f3=58 n3=20 |
    transp plane=13 |
    cat ${SOURCES[1]} axis=4 |
    transp plane=24 | reverse which=2 |
    linear o1=5745 d1=10 n1=100 niter=5 rect1=2 |
    transp plane=24 |
    clip2 lower=0 |
    put d2=1 d3=1
    ''')
  # Interpolate gas saturation files in x-y direction
```

```
Flow(tmp+'-int',tmp+'-int1 grid',
   '''
   transp plane=13 |
   iwarp2 warp=${SOURCES[1]} eps=.1
   n1=119 d1=80 o1=339532
   n2=135 d2=90 o2=1166840 |
   transp plane=13 | spline o1=5745 d1=5 n1=200 |
   clip2 lower=0
   ''')

# Regrid the interpolated gas saturation files in z direction
Flow(tmp+'-regrid1',[tmp+'-int'],
   '''
   window n3=1 | put o3=339442 |
   cat $SOURCE axis=3 |
   transp plane=13 memsize=1000 |
   spline o1=339504 d1=5 n1=1909 |
   transp plane=13  memsize=1000 | clip2 lower=0 |
   put d3=1 o3=330 | sfwindow min3=410 | pad end3=731
   ''')

# Regrid the interpolated files in x-y direction
Flow(tmp+'-regrid',tmp+'-regrid1',
   '''
   window max2=1174526 | transp memsize=1000 |
   spline o1=1166840 d1=40 n1=192 |
   clip2 lower=0 |
   pad beg1=17 | put o1=1 d1=1 |
```

```
    window n1=195 |
    transp memsize=1000 | transp plane=23 memsize=1000 |
    pad beg1=1149 end1=252 | put d1=.005
    ''')
# Write regridded gas saturation simulation files into directory "SEGYs"
Flow('./SEGYs/'+tmp+'-pCO2.sgy',[tmp+'-regrid','zheader'],'segywrite tfile=${SOURCES[1]}')
# Plot 3D gas saturation with faces corresponding to ccs1 (injection well)
# cmap3.csv is a color map file generated for custom color scale
Plot(tmp+'-3d-co2-ccs1',[tmp+'-regrid', 'cmap3.csv'],
     '''
     window min1=5.5 max1=7 min2=500 n2=1450 n3=195 |
     put o1=5000 d1=5 | transp plane=23 memsize=500 |
     byte gainpanel=all allpos=1 clip=.7 bar=trash8%s.rsf mean=y |
     grey3 title="%s CO\\_\s75 2\\^ \s100 Concentration" flat=n
     frame1=120 frame3=473 frame2=83 point1=0.75 point2=0.75
     scalebar=y color=${SOURCES[1]} maxval=.7
     label1=Depth unit1=ft unit2="" unit3= barlabel="Concentration"
     labelsz=10 labelfat=6 titlefat=8
     ''' % (str(i), year[i]))
pco2.append(tmp+'-3d-co2-ccs1') # append to 3D plot array
# plot 3D gas saturation with faces corresponding to VW1 well (monitoring well)
Plot(tmp+'-3d-co2-vw1',[tmp+'-regrid','cmap3.csv'],
     '''
     window min1=5.5 max1=7 min2=500 n2=1450 n3=195 |
     put o1=5000 o1=5 | transp plane=23 memsize=500 |
     byte gainpanel=all allpos=1 clip=.7 bar=trash9%s.rsf mean=y |
     grey3 title="%s CO\\_\s75 2\\^ \s100 Concentration" flat=n
     frame1=120 frame3=679 frame2=83 point1=0.75 point2=0.75
```

```
    scalebar=y color=${SOURCES[1]} maxval=.7
    label1=Depth unit1=ft unit2="" unit3= barlabel="Concentration"
    labelsz=10 labelfat=6 titlefat=8
    ''' % (str(i), year[i]))
pco22.append(tmp+'-3d-co2-vw1') # append to vw1 well plot array

# Plot gas saturation curve from simulation file corresponding to CCS1 well (injection well)
Plot(tmp+'-profile-ccs1',tmp+'-regrid',
  '''
  window n3=1 f3=83 n2=1 min2=973 min1=5.5 max1=7 |
  graph transp=y yreverse=y max2=1 title="%s"
  label1=Depth unit1=kft label2="CO\\_\s75 2\\^ \s100 Concentration"
  labelsz=10 labelfat=6 titlefat=8 screenwd=3 xll=2 yll=2

  ''' % year[i])
ccs1.append(tmp+'-profile-ccs1') # append to ccs1 well plot array

# plot gas saturation curve corresponding to VW1 well (monitoring well)
Plot(tmp+'-profile-vw1',tmp+'-regrid',
  '''
  window n3=1 f3=83 n2=1 min2=1179 min1=5.5 max1=7 |
  graph transp=y yreverse=y max2=1 title="%s"
  label1=Depth unit1=kft label2="CO\\_\s75 2\\^ \s100 Concentration"
  labelsz=10 labelfat=6 titlefat=8 screenwd=3 xll=2 yll=2
  '''%year[i])
vw1.append(tmp+'-profile-vw1') # append to vw1 well plot array

i += 1 # increment index
```

```
# plot baseline co2 with faces corresponding to ccs1 well
Plot('bpco2-3d','Jan2020-regrid cmap3.csv',
   '''
   window min1=5.5 max1=7 min2=500 n2=1450 n3=195 |
   math output=0 | put o1=5000 d1=5 | transp plane=23 memsize=500 |
   byte gainpanel=all mean=n allpos=n pclip=100 bar=trash11%s.rsf |
   grey3 title="Baseline CO\\_\s75 2\\^ \s100 Concentration"
   flat=n frame1=120 frame3=473 frame2=83 point1=0.75 point2=0.75
   scalebar=y color=${SOURCES[1]}  pclip=100
   label1=Depth unit1=ft unit2="" unit3= barlabel="Concentration"
   labelsz=10 labelfat=6 titlefat=8
   '''% str(i))
pco2.insert(0,'bpco2-3d')

# plot baseline co2 with faces corresponding to VW1 well
Plot('bpco2-3d2','Jan2020-regrid cmap3.csv',
   '''
   window min1=5.5 max1=7 min2=500 n2=1450 n3=195 |
   math output=0 | put o1=5000 d1=5 | transp plane=23 memsize=500 |
   byte gainpanel=all mean=n allpos=n pclip=100 bar=trash22%s.rsf |
   grey3 title="Baseline CO\\_\s75 2\\^ \s100 Concentration"
   flat=n frame1=120 frame3=679 frame2=83 point1=0.75 point2=0.75
   scalebar=y color=${SOURCES[1]}  pclip=100
   label1=Depth unit1=ft unit2="" unit3= barlabel="Concentration"
   labelsz=10 labelfat=6 titlefat=8
   '''% str(i))
pco22.insert(0, 'bpco2-3d2')
```

```
Result('pco2-3d',pco2,'TwoRows') # plot 3D gas saturation for all years (CCS1 well )
Result('pco2-3d2',pco22,'TwoRows') # plot 3D gas saturation for all years (VW1 well)
Result('ccs1-profile',ccs1,'TwoRows') # plot gas saturation curve for all years (CCS1 well)
Result('vw1-profile',vw1,'TwoRows') # plot gas saturation curve for all years (VW1 well)

###############################################################################
Uniform Saturation
###############################################################################

# loop over simulation files
for file in files:
  name = file[15:-4] # from the character length
  # estimate fluid density
  Flow(name+'_rho_fluid',name+'-regrid',
    '''
    math pco2=$SOURCE
    output="pco2*%f+(1-pco2)*%f"
    ''' % (moduli['CO2']['rho'],moduli['Brine']['rho']))

  # Estimate fluid bulk modulus
  Flow('K_'+name,name+'-regrid',
    '''
    math pco2=$SOURCE
    output="1/((pco2/%f)+((1-pco2)/%f))"
    ''' % (moduli['CO2']['K'],moduli['Brine']['K']))
```

```
# Estimate fluid saturated density
Flow('rho_'+name,['rho_min',name+'_rho_fluid','phi'],
   '''
   math rm=${SOURCES[0]} rf=${SOURCES[1]} phi=${SOURCES[2]}
   output="(1-phi)*rm+phi*rf"
   ''')
# Estimate fluid saturated bulk modulus
Flow('K_sat_'+name,['K_stiff', 'K_min', 'phi', 'K_'+name],
   '''
   math kd=${SOURCES[0]} km=${SOURCES[1]}
   phi=${SOURCES[2]} kf=${SOURCES[3]}
   output="kd+((1-kd/km)^2/(phi/kf+(1-phi)/km-kd/km^2+1e-10))"
   ''')
# Estimate fluid saturated Vp
Flow('vp_'+name,['K_sat_'+name, 'mu_stiff', 'rho_'+name],
   '''
   math ks=${SOURCES[0]} mu=${SOURCES[1]} rho=${SOURCES[2]}
   output="sqrt((ks+4/3*mu)/rho)"
   ''')
# Estimate fluid saturated AI
Flow('ai_'+name,['vp_'+name, 'rho_'+name],'mul ${SOURCES[1]}')
# Estimate fluid saturated reflectivity
Flow('monitor_'+name,['ai_'+name, 'vp_'+name, 'wavelet.rsf'],
   '''
   ai2refl | put d1=5 unit1=ft |
   depth2time velocity=${SOURCES[1]}
   nt=%d dt=.002 t0=0 |
   convft other=${SOURCES[2]} |
```

```
        window f1=550 n1=%d |
        put unit1=s
        '''% (nt, nt))
    # Write modeled time-lapse seismic data into directory "SEGYs"
    Flow('./SEGYs/'+name+'-monitor-uniform.sgy',['monitor_'+name, 'theader'],'segywrite tfile=${SOURCES[1]}')

    # Vp in kft/s for converting time to depth
    Flow('vp_kft_'+name,'vp_'+name,'add scale=.001')
    # convert modeled time-lapse seismic data from time to depth
    Flow('mon_depth_'+name,['monitor_'+name, 'vp_kft_'+name],'time2depth velocity=${SOURCES[1]} | put unit1=kft')
    # estimate the time lapse difference (in time)
    Flow('diff_'+name,['baseline', 'monitor_'+name],'add scale=-1,1 ${SOURCES[1]}')
    # estimate the time lapse difference (in depth)
    Flow('diff_depth_'+name,['baseline_depth', 'mon_depth_'+name],'add scale=-1,1 ${SOURCES[1]}')

#####################################################################################
Patchy Saturation
#####################################################################################

# loop over simulation files
for file in files:
    name = file[15:-4]
    # estimate fluid bulk modulus (pathcy)
    Flow('Kp_'+name,[name+'-regrid.rsf','mu_stiff'],
        '''
        math pco2=${SOURCES[0]} md=${SOURCES[1]}
        output="(pco2/(%f+(4/3)*md)+(1-pco2)/(%f+(4/3)*md))^(-1)-((4/3)*md)"
```

```
    '''% (moduli['CO2']['K'],moduli['Brine']['K']))

# estimate fluid saturated bulk modulus (patchy)
Flow('K_satp_'+name,['K_stiff', 'K_min', 'phi', 'Kp_'+name],
    '''
    math kd=${SOURCES[0]} km=${SOURCES[1]}
    phi=${SOURCES[2]} kf=${SOURCES[3]}
    output="kd+((1-kd/km)^2/(phi/kf+(1-phi)/km-kd/km^2+1e-10))"
    ''')
# Estimate fluid saturated Vp (patchy)
Flow('vpp_'+name,['K_satp_'+name, 'mu_stiff', 'rho_'+name],
    '''
    math ks=${SOURCES[0]} mu=${SOURCES[1]} rho=${SOURCES[2]}
    output="sqrt((ks+4/3*mu)/rho)"
    ''')
# estimate fluid saturated AI (patchy)
Flow('aip_'+name,['vpp_'+name, 'rho_'+name],'mul ${SOURCES[1]}')
# estimate fluid saturated reflectivity (patchy)
Flow('monp_'+name,['aip_'+name, 'vpp_'+name, 'wavelet.rsf'],
    '''
    ai2refl | put d1=5 unit1=ft |
    depth2time velocity=${SOURCES[1]}
    nt=%d dt=.002 t0=0 |
    convft other=${SOURCES[2]} |
    window f1=550 n1=%d |
    put unit1=s
    '''% (nt, nt))
# write modeled time-lapse seismic data data into directory "SEGYs"
```

```
    Flow('./SEGYs/'+name+'-monitor-patchy.sgy',['monp_'+name, 'theader'],'segywrite tfile=${SOURCES[1]}')
    # Vp in kft/s for converting time to depth
    Flow('vpp_kft_'+name,'vpp_'+name,'add scale=.001')
    # convert modeled time-lapse seismic data from time to depth
    Flow('monp_depth_'+name,['monp_'+name, 'vpp_kft_'+name],'time2depth velocity=${SOURCES[1]} | put unit1=kft')

    # estimate the time lapse difference (in time)
    Flow('diffp_'+name,['baseline', 'monp_'+name],'add scale=-1,1 ${SOURCES[1]}')
    # estimate the time lapse difference (in depth)
    Flow('diffp_depth_'+name,['baseline_depth', 'monp_depth_'+name],'add scale=-1,1 ${SOURCES[1]}')

######################Plotting Uniform Saturation ##################################

# plot baseline 3D seismic cube
Plot('baseline_3d','baseline',
    '''
    window min1=.8 max1=1.3 min2=500 n2=1450 n3=195 |
    transp plane=23 memsize=1000 |
    byte gainpanel=all bar=trash33%s.rsf  clip=1 |
    grey3 title="Baseline" flat=n frame1=225
    frame3=473 frame2=83 point1=.7 point2=0.7
    scalebar=y barlabel=Amplitude color=seismic
    label1=Time unit1=s minval=-1 maxval=1
    labelsz=10 titlefat=5 labelfat=4
    '''%str(i))

# plot baseline 2D seismic plane (corresponidng to both CCS1 and VW1 well locations)
```

```
Plot('baseline_2d','baseline',
   '''
   window min1=0.6 n3=1 f3=84 |
   grey title="Baseline" color=seismic
   scalebar=y barlabel=Amplitude
   label1=Time unit1=s uni2= label2=Crossline
   wheretitle=t wherexlabel=b minval=-.8 maxval=.8 clip=.8
   ''')

# plot baseline AI cube
Plot('baseline_ai','ai',
   '''
   put d1=0.005 |
   window min1=4.5 min2=700 max2=1200 min3=50 max3=120|
   byte gainpanel=all allpos=n mean=y bar=trash44%s.rsf |
   grey3 title="Baseline" flat=n frame1=435
   frame2=273 frame3=34 point1=0.75 point2=0.75
   scalebar=y color=roma barlabel="Acoustic Impedance"
   label1=Depth unit1=kft
   '''%str(i))

data3d = ['baseline_3d'] # array for 3D seismic differnece plots
data2d = ['baseline_2d'] # array for 2D seismic difference plots
ai3d = ['baseline_ai'] # array for AI difference plots
mon3d = ['baseline_3d'] # array for monitor 3D plots

for i, file in enumerate(files):
   name = file[15:-4]
```

```
# plot 3D seismic difference
Plot(name+'_3d','diff_'+name,
   '''
   window min1=.8 max1=1.3 min2=500 n2=1450 n3=195 |
   transp plane=23 memsize=1000 |
   byte gainpanel=all bar=trash55%s.rsf clip=0.2 |
   grey3 title="%s Monitor - Baseline" flat=n
   frame1=225 frame3=473 frame2=83 point1=0.7 point2=0.7
   scalebar=y barlabel="Amplitude Difference"
   label1=Time unit1=s  color=seismic
   minval=-0.09 maxval=0.09
   labelsz=10 titlefat=5 labelfat=4
   ''' % (str(i), year[i]))
# plot 3D modeled time-lapse seismic data
Plot(name+'_3d_mon','monitor_'+name,
   '''
   window min1=.8 max1=1.3 min2=500 n2=1450 n3=195 |
   transp plane=23 memsize=1000 |
   byte gainpanel=all bar=trash66%s.rsf clip=1 |
   grey3 title="%s Monitor" flat=n
   frame1=225 frame3=473 frame2=83 point1=0.7 point2=0.7
   scalebar=y barlabel="Amplitude"
   label1=Time unit1=s  color=seismic
   minval=-1 maxval=1
   labelsz=10 titlefat=5 labelfat=4
   ''' % (str(i), year[i]))
# plot 2D seismic difference
Plot(name+'_2d','diff_'+name,
```

```
      '''
      window min1=.6 n3=1 f3=84 |
      grey title="%s Monitor - Baseline"  color=seismic
      scalebar=y barlabel="Amplitude Difference"
      label1=Time unit1=s uni2= label2=Crossline color=seismic
      wheretitle=t wherexlabel=b clip=.2 minval=-.2 maxval=.2
      ''' % year[i])
    # Window AI difference
    Flow(name+'_ai_diff',['ai_'+name,'ai'],
      '''
      add scale=1,-1 ${SOURCES[1]} |
      put d1=0.005 |
      window min1=4.5 min2=700 max2=1200 min3=50 max3=120
      ''')
    # plot AI difference
    Plot(name+'_ai',name+'_ai_diff',
      '''
      add scale=-1 |
      byte gainpanel=all color=j clip=2500 bar=trash77%s.rsf mean=y allpos=y |
      grey3 title="%s Monitor - Baseline" flat=n frame1=425
      frame2=273 frame3=34 point1=0.75 point2=0.75
      scalebar=y color=inferno barlabel="Acoustic Impedance Difference"
      label1=Depth unit1=kft minval=0 maxval=-2500
      ''' % (str(i) , year[i]))
    data3d.append(name+'_3d')   # append to 3D seismic difference array
    mon3d.append(name+'_3d_mon') # append to 3D monitor array
    data2d.append(name+'_2d')   # append to 2D seismic difference array
    ai3d.append(name+'_ai')    # append to AI difference array
```

```
Result('3D_Uniform',data3d,'TwoRows') # plot 3D seismic difference for all years
Result('2D_Uniform',data2d,'TwoColumns') # plot 2D seismic difference for all years
Result('ai_Uniform',ai3d,'TwoColumns') # plot AI difference for all years
Result('mon_Uniform',mon3d,'TwoRows') # plot 3D monitor for all years

##################### Plotting Patchy Saturation ################################

data3d = ['baseline_3d']    # array for 3D seismic difference plots
data2d = ['baseline_2d']    # array for 2D seismic difference plots
ai3d = ['baseline_ai']    # array for AI difference plots
mon3d = ['baseline_3d']   # array for monitor 3D plots

# loop over simulation files
for i, file in enumerate(files):
   name = file[15:-4]
   # plot 3D seismic difference
   Plot(name+'_3dp','diffp_'+name,
      '''
      window min1=.8 max1=1.3 min2=500 n2=1450 n3=195 |
      transp plane=23 memsize=1000 |
      byte gainpanel=all bar=trash88%s.rsf clip=0.2 |
      grey3 title="%s Monitor - Baseline" flat=n
      frame1=225 frame3=473 frame2=83 point1=0.7 point2=0.7
      scalebar=y barlabel="Amplitude Difference"
      label1=Time unit1=s  color=seismic
      minval=-0.09 maxval=0.09
      labelsz=10 titlefat=5 labelfat=4
```

```
    ''' % (str(i), year[i]))
# plot 3D monitor
Plot(name+'_3d_monp','monp_'+name,
    '''
    window min1=.8 max1=1.3 min2=500 n2=1450 n3=195 |
    transp plane=23 memsize=1000 |
    byte gainpanel=all bar=trash99%s.rsf clip=1 |
    grey3 title="%s Monitor" flat=n
    frame1=225 frame3=473 frame2=83 point1=0.7 point2=0.7
    scalebar=y barlabel="Amplitude"
    label1=Time unit1=s  color=seismic
    minval=-1 maxval=1
    labelsz=10 titlefat=5 labelfat=4
    ''' % (str(i), year[i]))
# plot 2D seismic difference
Plot(name+'_2dp','diffp_'+name,
    '''
    window min1=.6 n3=1 f3=84 |
    grey title="%s Monitor - Baseline" color=seimsic
    scalebar=y barlabel="Amplitude Difference"
    label1=Time unit1=s uni2= label2=Crossline color=seismic
    wheretitle=t wherexlabel=b clip=.2 minval=-.2 maxval=.2
    ''' % year[i])
# Window AI difference
Flow(name+'_aip_diff',['aip_'+name,'ai'],
    '''
    add scale=1,-1 ${SOURCES[1]} |
    put d1=0.005 |
```

```
        window min1=4.5 min2=700 max2=1200 min3=50 max3=120
        ''')
    # plot AI difference
    Plot(name+'_aip',name+'_aip_diff',
        '''
        add scale=-1 |
        byte gainpanel=all color=j clip=2500 bar=trash111%s.rsf mean=y allpos=y |
        grey3 title="%s Monitor - Baseline" flat=n frame1=425
        frame2=273 frame3=34 point1=0.75 point2=0.75
        scalebar=y color=inferno barlabel="Acoustic Impedance Difference"
        label1=Depth unit1=kft minval=0 maxval=-2500
        ''' % (str(i), year[i]))
    data3d.append(name+'_3dp')  # append to 3D seismic difference array
    data2d.append(name+'_2dp')  # append to 2D seismic difference array
    ai3d.append(name+'_aip')    # append to AI difference array
    mon3d.append(name+'_3d_monp')   # append to 3D monitor array

Result('3D_Patchy',data3d,'TwoRows')    # plot 3D seismic difference for all years
Result('2D_Patchy',data2d,'TwoColumns') # plot 2D seismic difference for all years
Result('ai_Patchy',ai3d,'TwoColumns')   # plot AI difference for all years
Result('mon_Patchy',mon3d,'TwoRows')    # plot 3D monitor for all years
```